Probing functional and optical cross-sections of PSII in leaves during state transitions using fast repetition rate light induced fluorescence transients

Barry Osmond [1, 2, 3], Wah Soon Chow [2], Barry J Pogson [2], Sharon A Robinson [1]

[1] Centre for Sustainable Ecosystem Solutions, School of Biological Sciences, University of Wollongong, Northfields Ave., Wollongong, NSW 2522, Australia

[2] Division of Plant Sciences, Research School of Biology, The Australian National University, 46 Sullivan's Creek Road, Acton, ACT 2601, Australia

[3] Corresponding author; PO Box 3252 Weston Creek, ACT 2611, Australia

osmond.barry@gmail.com

Keywords: Arabidopsis mutants; barley mutants; chlorophyll fluorescence, electron transfer rates; PQ pool redox status

Abstract: (396 words)

Plants adjust the relative sizes of PSII and PSI antennae in response to the spectral composition of weak light favouring either photosystem by processes known as state transitions (ST) attributed to a discrete antenna migration involving phosphorylation of light-harvesting chlorophyll-protein complexes in PSII. Here for the first time we monitor the extent and dynamics of ST in leaves from estimates of optical absorption cross-section (relative PSII antenna size; a_{PSII}). These estimates are obtained from in situ measurements of functional absorption cross-section (σ_{PSII}) and maximum photochemical efficiency of PSII (ϕ_{PSII}); i.e., $a_{PSII} = \sigma_{PSII} / \phi_{PSII}$ (Kolber *et al.* 1998) and other parameters from a Light Induced Fluorescence Transient (LIFT) device (Osmond *et al.* 2017). The Fast Repetition Rate (FRR) Q_A flash protocol of this instrument monitors chlorophyll fluorescence yields with reduced Q_A irrespective of the redox state of PQ, as well as during strong ~1 s white light pulses that fully reduce the PQ pool. Fitting this transient with the FRR model also monitors ETR kinetics from PSII → PQ, PQ → PSI, and the redox state of the PQ pool in the "PQ pool control loop" that underpins ST, with a time resolution of a few seconds. All LIFT/FRR criteria confirm the absence of state transitions in antenna mutants *chlorina-f*2 of barley and *asLhcb*2-12 of *Arabidopsis* as well as its STN7 kinase mutants *stn7* and *stn7/8*. In contrast, wild type barley and *Arabidopsis* genotypes *Col*, *npq*1, *npq*4, *OEpsbs*, *pgr*5 *bkg*, and *pgr5*, show normal ST but the extent of ST (and by implication, the size of the phosphorylated LHCII pool participating in ST) deduced from changes in a'_{PSII} and other parameters with reduced Q_A range up to 35% whereas estimates from strong WL pulses in the same assay are only ~10%. Despite the absence of ST, *asLhcb*2-12 displays normal wild type modulation of ETR and the PQ pool during assays. Distinctively, when LHCII phosphorylation is impaired in *stn7* and *stn7/8* the Q_A flash and WL pulse produce similar fluorescence yields, and accelerated ETR results in a persistently over-reduced PQ pool in

these genotypes. The larger estimates of ST from the Q_A flash and anomalous fluorescence yields in kinase mutants are discussed in the context of contemporary dynamic structural models of ST involving formation and participation of PSII and PSI megacomplexes in an 'energetically connected lake' of free phosphorylated LHCII trimers (Grieco *et al.* 2015).

Abbreviations (see also Table 1; Osmond *et al.* 2017)

EST PAM	= $F'_m PAM^{470+740} / F'_m PAM^{470}$; extent of ST from spot measurements of F'_m with fully reduced PQ during the saturating WL pulse (0.8 s) of PAM in light 2 (470 nm) at steady state and shortly after removal of added light 1 (740 nm).
EST WL	= $F'_m WL^{470+740} / F'_m WL^{470}$; extent of ST from spot measurements of $F'_m WL$ with fully reduced PQ monitored by the Q_A flash of LIFT/FRR during ~1 s PAM-analogous WL pulses in light 2 at steady state and shortly after removal of added light 1
EST Q_A	= $F'_m Q_A^{470+740} / F'_m Q_A^{470}$; extent of ST from the average of ~20 measurements of $F'_m Q_A^{470}$ in light 2 at steady state and maximum $F'_m Q_A^{470+740}$ after removal of added light 1
$EST\sigma'_{PSII}$	= $\sigma'_{PSII}{}^{470+740}/\sigma'_{PSII}{}^{470}$; extent of ST from the average of ~20 Q_A measurements of σ'_{PSII} in light 2 and after removal of added light 1
$EST\ a'_{PSII}$	= $a'_{PSII}{}^{470+740} / a'_{PSII}{}^{470}$; extent of ST from ~20 Q_A flash averaged measurements of σ'_{PSII} and ϕ'_{PSII} (from $F'_m WL$ and $F'Q_A$ in strong WL pulses) in light 2 and after removal of added light 1, used to calculate $a'_{PSII} = \sigma'_{PSII} / \phi'_{PSII}$
E_k	FRR model simulated half saturation PFD for photosynthetic electron transport
FRR	fast repetition rate protocol and model fit to chlorophyll fluorescence transient
LHCII	light-harvesting chlorophyll-protein complexes with PSII (or LHCI with PSI)
(P)LHCII	phosphorylated light-harvesting chlorophyll-protein complexes with PSII
LIFT	light induced fluorescence transient (device)
Light 1	740 nm LED; light preferentially absorbed by photosystem I
Light 2	470 nm LED; light preferentially absorbed by photosystem II
NIR	near infra red light (e.g., 700-750 nm)
PAM	pulse amplitude modulated (fluorometer)
PQ_{OX}	relative oxidation status of the PQ pool
RCII	reaction centre of PSII
ST	state transition; ST+ = ST competent (present); ST- = ST incompetent (absent)
S1	state 1
S2	state 2
WL	white light, 400 - 655 nm; filtered from a quartz iodide lamp

Introduction

Since Bonaventura and Myers (1969) and Murata (1969, 2009) a diverse array of experiments show that photosynthetic cells adjust the relative sizes and functions of PSII and PSI antennae in response to the spectral composition of light by processes known as state transitions (ST). Initially based on observations of chlorophyll fluorescence emission spectra and kinetics, subsequent studies of light-dependent phosphorylation of light-harvesting chlorophyll-protein complexes in chloroplast membranes (Bennett *et al.*1980, Allen *et al.* 1981; Allen 2002) led to a discrete antenna migration model for ST (Fig. 1*a*). In the dark or in the presence of light predominantly absorbed by PSI (light 1; e.g., λ 740 nm LED, or natural canopy shade enriched in NIR) leaves are in state 1 (S1) in which LHCIIs are predominantly associated with PSII, yielding higher levels of fluorescence. Over-excitation of the photosynthetic apparatus with light predominantly absorbed by PSII (light 2; e.g., λ 470nm) causes reduction of thylakoid PQ pools and initiates transition from state 1 to state 2 (S2) by activation of kinases that phosphorylate and mobilise a fraction of (P)LHCIIs from PSII and become associated with PSI, leading to a lower yield of chlorophyll fluorescence from PSII at room temperature. Transition back to S1 is initiated when PSI is over-excited in light 1 (e.g., λ 740 nm), the PQ pool becomes more oxidised, kinases are inhibited and phosphatases are activated. These de-phosphorylate (P)LHCIIs in PSI antennae that then re-associate with PSII leading to a higher yield of chlorophyll fluorescence. For convenience, the biochemistry underlying the antenna migration model is referred to as a "PQ pool/ST control loop".

Following the prescient conclusion of Wang and Myers' (1974) that 'the absorption cross-section for System II is indeed higher in State 1 than in State 2', cross-section terminology has been applied to a range of functional and structural changes occurring during ST (Horton 1983, Allen and Melis 1988, Tikkanen *et al.* 2008, Ruban and Johnson 2009; Allen 2017). This usage generally refers to changes in optical absorption cross-sections (apparent antenna size) of PSII and PSI inferred from changes in chlorophyll fluorescence from LHCIIs at room

109 temperature, or from both photosystems measured at 77ºK. It is now supported by a plethora of
110 insight into structural / functional aspects of ST from selective release of (P)LHCII complexes in
111 thylakoids of from algae and leaves by mechanical and detergent methods (Iwai *et al.* 2008; Järvi
112 *et al.* 2011; Minagawa 2011; Galka *et al.* 2012; Rantala *et al.* 2017). These are leading to major
113 re-evaluation of the functional significance of the discrete antenna migration model. For example,
114 Grieco *et al.* (2015) point out that this model 'completely fails to explain the physiological
115 significance of steady state phosphorylation of LHCII in all thylakoid domains under any constant
116 light condition'.

117 The discrete phosphorylation of LHCIIs associated with PSII centres proposed in the
118 antenna migration model for ST in Fig. 1*a* now has to be accommodated in the context of a
119 'LHCII connectivity model' (Grieco *et al.* 2015) in which up to 50% of the (P)LHCII pool (Galka
120 *et al.* 2012) is loosely associated with PSII centres. Furthermore, in one view (Galka *et al.* 2012;
121 Wientjes *et al.* 2013*b*), megacomplexes are formed by recruitment of these 'extra (P)LHCIIs' to
122 PSI centres, and Yokono *et al.* (2015) report 'about half of PSIIs are connected to PSIs in
123 *Arabidopsis*'. Live cell imaging of ST in *Chlamydomonas reinhardtii* (Iwai *et al.* 2010) and
124 *Arabidopsis* (Kim *et al.* 2015 *et al.* 2017) suggest that PSII-LHCII-PSI megacomplexes allow 'a
125 fluent and balanced electron transfer between PSII and PSI' (Mekala *et al.* 2015) via from
126 multiple antennae (Bos *et al.* 2017). The core components of the "PQ pool/ST control loop" in
127 Fig. 1*a* represent 'only a part of a larger megacomplex that accounts for energy distribution
128 between PSII and PSI' (Rantala *et al.* 2017).

129 Chlorophyll fluorescence assays of the functional absorption cross-section of PSII (σ_{PSII})
130 in *Chlorella* (Ley and Mauzerall 1982) led to fast repetition rate fluorometers (FRRf) capable of
131 monitoring this parameter in phytoplankton in the field (Behrenfeld and Kolber 1999) and
132 laboratory (Suggett *et al.* 2004) and have supported holistic evaluation of ST in microalgae.
133 Especially relevant to the present report is the monitoring of σ_{PSII} in thylakoid particles

prepared from *Chlamydomonas reinhardtii* during ST (Iwai *et al.* (2008). When locked in S1, large particles (type I; LHCII replete ≥ 2,000 kD) with much higher σ'_{PSII} (366 ± 20 Å^2/RCII) predominate. When cells are locked in S2 smaller particles are obtained (Type III; LHCII depleted ~ 300-400 kD) and have smaller σ'_{PSII} = 163 ± 88 Å^2/RCII. Kolber *et al.* (1998) show that optical absorption cross-section (a_{PSII}; apparent antenna size) can be estimated from contiguous measurements of σ_{PSII} and maximum photochemical efficiency of PSII (ϕ_{PSII}); i.e., a_{PSII} = σ_{PSII} / ϕ_{PSII} (in the dark) and a'_{PSII} = σ'_{PSII} / ϕ'_{PSII} (in the light).

Such measurements are now are accessible in leaves in situ using LIFT/FRR instruments and techniques (http://soliense.com/LIFT_Method.php; accessed 28-12-2018) at distances up to 40 m (Kolber *et al.* 2005). Compared to wild types, estimates of a_{PSII} in small antenna mutants of *Arabidopsis* (*asLhcb*2-12) and barley (*chlorina-f2*) are similar (Osmond *et al.* 2017) to independent in vitro estimates of this property reported in the literature (Andersson *et al.* 2003; Harrison *et al.* 1993; Bossmann *et al.* 1997). Moreover wild type *Arabidopsis*, barley and spinach show the expected decline in σ_{PSII} and a_{PSII} with increasing growth irradiance (Osmond *et al.* 2017). Differences in a_{PSII} now are detectable to within a few percent and thus seem sufficiently sensitive for quantifying apparent PSII antenna size during ST.

We posit that it now is time to monitor ST directly through measurements of functional and optical cross-sections. Three specific objectives of this paper are:

(i) to validate the LIFT/FRR approach for monitoring changes in relative PSII antenna size (a'_{PSII}) ST competent genotypes and ST mutants of barley and *Arabidopsis* assayed under artificial but well defined conditions in light 2 and light 2+1,

(ii) to compare the estimates of mobilizable PSII antenna LHCIIs implied from chlorophyll fluorescence monitored by LIFT/FRR with reduced Q_A to those obtained in traditional assays using a strong WL pulse with fully reduced PQ.

158 *(iii)* to concurrently monitor the PQ pool redox state and associated ETR parameters
159 deemed to initiate and regulate ST in situ.
160 In general, these objectives are pursued in terms of the antenna migration model but also
161 are discussed in the context of contemporary evidence that it is just one component of processes
162 balancing the excitation load between PSII and PSI in situ (Rantala *et al.* 2017).
163

164 ## Materials and methods

165 ### *Plant material*

166 Wild type barley (*Hordeum vulgare* L.), and its Chl *b*-less mutant *chlorina-f*2 (Highkin 1950),
167 were grown in full sunlight, side by side, in a south-facing temperature-controlled (25 ºC day/15
168 ºC night) greenhouse. The mid-section of attached leaves, or leaf segments cut under, and
169 kept in, a small trough of water were arranged vertically in one or two layers to maximize
170 chlorophyll fluorescence yield from the LIFT excitation spot during the PAM-analogous
171 assays described below.
172 Arabidopsis (*Arabidopsis thaliana* L. Heynh.) genotypes were cultivated in controlled
173 environment growth chambers (20 ºC; at ~120 µmol photons m^{-2} s^{-1}). Six ST competent (ST+)
174 genotypes were studied; including two wild types *Col* and *pgr*5 *bkg* and PsbS protein over
175 expressor *OEpsbs* (Li *et al.* 2002), as well as three NPQ mutants *npq*1 (Niyogi *et al.* 1998), *npq*4
176 (ΔpH sensing PsbS protein; Li *et al.* 2000) and *pgr*5 (cyclic electron transport deficient;
177 Munekage *et al.* 2002). They were compared with three ST incompetent genotypes (ST-)
178 including smaller antenna mutant *asLhcb*2-12, almost completely devoid of Lhcb1 and Lhcb2
179 (Andersson *et al.* 2003; identified as *ant*ST-) and STN7 kinase mutants (identified as *kin*ST-)
180 *stn*7 (Bellafiore *et al.* 2005) and *stn*7/8 (Bonardi *et al.* 2005). All genotypes were grown at the
181 same time under the same conditions and selected randomly for a total of 21 assays over a period
182 of three days.

The LIFT apparatus and FRR protocols

All data in this report are derived from the prototype bench-top, limited-range version of LIFT equipped with an eye-safe blue LED (λ 470 nm), and are based on the Q_A flash protocol described previously (Osmond *et al.* 2017). Additional technical information is available at http://soliense.com/LIFT_Terrestrial.php (accessed 13-07-18). Kolber *et al.* (1998) conclude that the lower limit of excitation power to reliably calculate photosynthetic parameters under conditions of negligible Q_A re-oxidation is about 1.6 quanta per RCII. The Q_A flash of LIFT/FRR elicits a transient increase in chlorophyll fluorescence from a 0.36 ms long saturation sequence (SQ_A) of 180 brief flashlets (1 µs; each ~13,000 µmol photons m^{-2} s^{-1}) that delivers an excitation power of 2.3 µmol 470 nm photons m^{-2}. In an average leaf with ~1 µmol RCII m^{-2} (WS Chow unpublished) more than half of these photons in each flashlet are absorbed by a RCII and achieve > 90% reduction of Q_A. At a distance of ~60 cm the Q_A flash protocol at 2 to 3 s intervals delivers a monitoring beam of ~1.2 µmol photons m^{-2} s^{-1} of light 2 (470 nm), comparable to that applied on-the-leaf at a distance of 1 mm by the monitoring beam of a JUNIOR-PAM at 100 Hz (Pfündel 2007).

Previous studies (Osmond *et al.* 2017) show that F_mQ_A from the Q_A flash on dark adapted spinach leaves is 63 ± 1% of F_mPQ compared to F_J / F_P = 55 ± 5% in Kautsky chlorophyll fluorescence induction curves on the same leaves in 3,000 µmol photons m^{-2} s^{-1} red light. The ratio F_mQ_A / F_mPQ was 0.59 ± 0.01 in the nine *Arabidopsis* genotypes assayed here, suggesting excitation power of the Q_A flash is adequate to elicit the fluorescence yield typical of the O-J component of the O-J-I-P fluorescence induction transient. The biophysical/biochemical background to the relationships between F_mQ_A and F_mPQ determined by LIFT/FRR now have been explored in detail with a commercially available instrument developed from this prototype, using different FRR protocols and parameter nomenclature (Keller *et al.* 2018).

The saturation phase of Q_A flash is followed by a relaxation sequence (RQ_A) of 90 flashlets of half intensity at exponentially increasing intervals over ~30 ms that monitors Q_A re-

209 oxidation as electrons are transferred to PSI. The entire chlorophyll fluorescence transient is fitted
210 with the FRR model to estimate functional and optical absorption cross-sections of PSII and to
211 characterise the properties of electron transport between PSII and PSI. The methodology,
212 assumptions and fitting procedures in this model are described in Kolber *et al.* (1998); see
213 also http://www.soliense.com/LIFT_Method.php (accessed 13-07-18).

214 The number of flashlets, their energy, and frequency are controlled by the LIFT software,
215 and FRR fitting and analysis of the fluorescence transient can be adjusted to optimize derivation
216 of the above parameters in the plant system under observation. For example, under some
217 experimental conditions a transient feature is observed ~15 ms into the RQ_A phase of the
218 chlorophyll fluorescence transient. It is indicative of PQ pool over reduction prior to the Q_A flash
219 (Osmond *et al.* 2017) and usually disappears with time after a strong WL pulse, but persists in
220 the STN7 kinase mutants of *Arabidopsis* examined here. In order to produce comparative
221 estimates of ETR and PQ redox properties between genotypes we confine the FRR fit to the first
222 10 ms of the 30 ms RQ_A phase.

223 ### *Notation for LIFT/FRR and estimating a'_{PSII} from σ'_{PSII} and ϕ'_{PSII}*

224 The notation applied to data collected by LIFT and processed by the FRR model is explicitly
225 devised to minimize ambiguity between LIFT/FRR and traditional PAM assays (Table 1 in
226 Osmond *et al.* 2017). For example, the lower maximum chlorophyll fluorescence yield attained
227 during continuous monitoring with the Q_A flash in the dark is distinguished as F_mQ_A (or F'_mQ_A
228 in the light). The higher fluorescence yield obtained in spot measurements with full reduction of
229 both Q_A and the PQ pools in a PAM-analogous strong WL pulse is identified by the postfix *WL*
230 (e.g., F_mWL and F'_mWL).

231 The maximum photochemical efficiency of PSII continuously monitored by the Q_A flash
232 with reduced Q_A:

233 $$\phi_{PSII}Q_A = (F_mQ_A - F_oQ_A)/F_mQ_A \text{ and } \phi'_{PSII}Q_A^{470} = (F'_mQ_A - F'Q_A)/F'_mQ_A \quad (1)$$

in the dark and light, respectively and are superscripted in light 2 as $\phi'_{PSII}Q_A^{470}$ and $\phi'_{PSII}Q_A^{470+740}$ in light 2+1.

These measurements are distinguished from data monitored in the Q_A flash during PAM-analogous strong WL pulses with a fully reduced PQ pool as:

$$\phi_{PSII}WL = (F_mWL - F_oQ_A) / F_mWL \text{ and } \phi'_{PSII}WL = (F'_mWL - F'Q_A) / F'_mWL \quad (2)$$

in the dark and light, respectively and are superscripted in light 2 as $\phi'_{PSII}WL^{470}$ and $\phi'_{PSII}WL^{470+740}$ in light 2+1.

Values of σ_{PSII} and σ'_{PSII} (functional absorption cross-section of PSII in the dark and in the light, respectively; in units of $Å^2$/RCII) are determined, to a first degree, by the initial slope of the Q_A flash transient but are calculated by fitting the entire fluorescence transient into the FRR model. The optical absorption cross-section (a_{PSII}, also in units of $Å^2$/RCII) quantifies the PSII-specific rates of light absorption. According to Falkowski and Kolber (1995; *Eq.* 8) and Kolber *et al.* (1998; *Eq. 12*, derived from *Eqs. 7 – 9*) these parameters are related by $\sigma_{PSII} = a_{PSII} \times \phi_{PSII}$ so estimates of the respective optical absorption cross-sections (apparent antenna sizes) in the dark are calculated from:

$$\sigma_{PSII} = \sigma_{PSII} / \phi_{PSII}WL \quad (3)$$

Because the ST assay used here provides strong WL pulses to obtain spot measurements of F'_mWL at steady state in each light treatment, we also have access to values of $\phi'_{PSII}WL$ after 10 min. in light 2 and shortly after removal of added light 1. In the absence of further theoretical and empirical evidence as to values of the photochemical efficiency of PSII in these light treatments, we estimate a'_{PSII} pragmatically as:

$$a'_{PSII} = \sigma'_{PSII} / \phi'_{PSII}WL \quad (4)$$

in the dark and light respectively, and values are superscripted in light 2 as $a'_{PSII}{}^{470}$ and $a'_{PSII}{}^{470+740}$ in light 2+1.

The RQ_A phase of the Q_A flash allows estimation of several time constants for electron transport and here the double-stage fitting procedure and underlying assumptions described in http://www.soliense.com/LIFT_Method.php (accessed 13-07-18) is used to obtain τ_1, the average time constants for $Q_A \rightarrow$ PQ electron transport, and τ_2, the time constant for PQ pool re-oxidation. It also provides estimates of the oxidized portion of the PQ pool (PQ_{OX}) and the ratio τ_2 / PQ_{OX} measures downstream electron transport rates from the PQ pool to PSI, all of which effectively monitor the "PQ pool/ST control loop". In total, data from ST assays used here are based on >20,000 Q_A flashes with a mean signal/noise ratio of 272 and an average Chi-squared fit of 2.85.

Light sources for laboratory ST assays

Weak light 2 (470 nm ~5 μmol photons m^{-2} s^{-1}) is supplied from the LIFT LED excitation source operating in DC mode to predominantly activate PSII (but see Laisk *et al.* 2014). The source of light 1 (740 nm ~50 μmol photons m^{-2} s^{-1}; with only 0.46% emission below 700 nm) is from an externally operated LED (LED735-66-60; 741 ±13 nm; Roithner LaserTecknic, Vienna, Austria). By chance, the intensity of light 1 compared to light 2 is similar to that of 645 nm light 2 and 710 nm light 1 used by Bonaventura and Meyers (1969) with *Chlorella*. A quartz iodide lamp in an externally controlled Rollei P355 slide projector fitted with a 400 - 655 nm cut-out filter (<1% transmission 700 - 890 nm; Ditric Optics #15-31690) is the source of strong, PAM-analogous WL pulses. White light and light 2 are measured on the leaf with calibrated LS-C mini-quantum sensors (400-700 nm) using a universal light meter ULM-500 (H Walz GmbH, Effeltrich, Germany). Light 1 is measured with a SKP 216-ER sensor; 550-750 nm (Skye Instruments, Llandrindod Wells, Powys LD1 6DF UK) and its spectral response checked with a LI-COR 1800 spectral radiometer (LI-COR Inc. Lincoln, NE 68504-0425 USA).

State transition assays

State transitions assays are initiated and quantified by adapting the artificial PAM procedure previously used in our laboratory following that used by Haldrup *et al.* (2001). It differs from that used by Ruban and Johnson (2009) in that the assays begin with dark to S2 rather than to S1. Figure 1*b* illustrates such a MINI-PAM assay with a spinach leaf (dark adapted ~30 min.). After a saturating pulse of WL (SP) to obtain F_mPAM in the dark it is followed ~1 min. later by exposure to weak light 2 for ~10 min. to induce S2, after which another SP is applied to estimate F'_mPAM^{470}. When the measuring beam signal returns to pre-pulse levels light 1 is added for a further 10 min. to induce S2→S1. Some 30 s later another SP is applied to obtain $F'_m{}^{470+740}PAM$. The extent of state transition is estimated as $EST_{PAM} = F'_mPAM^{470+740} / F'_mPAM^{470}$. Preliminary assays of *Arabidopsis* genotypes with MINI-PAM established *Col* is ST+ (EST_{PAM} = 1.12) whereas *asLhcb*2-12 (*ant*ST-) as well as *stn*7 and *stn*7/8 (*kin*ST-) have EST_{PAM} = 0.99 (means of duplicates) and are clearly ST-. When adapted for assays of ST with LIFT/FRR the above sequence proves to be logistically convenient for simultaneously switching the 470 nm LED delivering the Q_A flash to DC mode as a source of actinic light 2. Note that in both PAM and LIFT/FRR assays, weak light 2 is present throughout.

Results

Introducing the holistic LIFT/FRR state transition assay

Tikkanen and Aro (2014) highlight the potential pitfalls associated with chlorophyll fluorescence instruments that use monitoring beams with light predominantly exciting PSII, and LIFT/FRR is no exception in this respect. The balance of PSII and PSI excitation achieved in the 270 strong, but brief, flashlets (1 µs) of 470 nm (light 2) in the monitoring Q_A flashes of LIFT/ FRR delivers remarkably stable values of photosynthetic parameters in prolonged dark, but this steady state is extremely sensitive to low levels of near infra red light (e.g., from fluorescent laboratory lighting; Fig. 6*a* in Osmond *et al.* 2017). Consequently, care is needed

when interpreting fluorescence responses to addition of 740 nm light 1 to light 2 during the artificial ST assay.

Figure 2 shows kinetic profiles of parameters obtained in the course of a ST assay in *Arabidopsis* NPQ mutant *npq*1. This genotype is selected to illustrate the LIFT/FRR approach because there is minimal likelihood that non-photochemical quenching of chlorophyll fluorescence will complicate interpretation of fluorescence yields during the low intensity light treatments. Full annotation is provided as a prelude to subsequent representative kinetic profiles from wild types and ST mutants and illustrates the holistic array of parameters derived from FRR model fit to >900 individual Q_A flash transients applied throughout each ST assay. In addition kinetic profiles are colour-coded to facilitate interpretation of responses throughout the assay.

(i) Responses to light 1 in the dark

The LIFT/FRR assays of ST with dark adapted leaves (>30 min.) commence with brief exposure (~1 min.) to 740 nm light 1 to differentiates the above mentioned responses of the photosynthetic apparatus to NIR light from the slower, S2→S1 responses following addition of light 1 in presence of light 2. Light 1 produces an immediate decline in F_mQ_A (within the first few flashes) without change in F_oQ_A (Fig. 2*a*), so there is a relatively small decline in $\phi'_{PSII}Q_A$ (Fig. 2*b*), as confirmed in the solid black and red traces in the SQ_A phase of the Q_A flash fluorescence transient illustrate (Fig. 2*f*). The RQ_A phase of these transients shows slight acceleration in τ_1 and some slowing of τ_2 (Figs. 2*b, c, f*). The fast increase in relative oxidation state of the PQ pool on addition of light 1 (Fig. 2*c*) returns to the dark reduced state noticeably more slowly on removal of light 1. This evidently monitors the rapid re-poising of ETR following activation of an electron sink in PSI as confirmed by the ratio τ_2 / PQ_{OX} pool (a measure of electron transport rates from PQ pool to PSI, Fig. 2*d*) which rapidly accelerates on addition of light 1 and slows again on its removal. Exposure to light 1 in the dark also produces an immediate, and reversible ~20% increase in σ'_{PSII} (Fig. 2*e*).

These rapid responses, noted by Bonaventura and Meyers (1969) in their pioneering studies of ST, are attributed by them to 'the consequences of shifts in the concentration of open reaction centers of PSII induced by the addition and removal of the oxidizing effects of Photoreaction 1'. Dark adapted leaves of all species monitored by LIFT/FRR including barley *chlorina-f2* and *Arabidopsis* genotypes *asLhcb2-12*, *stn7* and *stn7/8* that lack ST, exhibit these fast transients on exposure to light 1, so they cannot be attributed to ST per se.

(ii) Evaluation the PAM-analogous strong WL pulse

The maximum photochemical efficiency of photosystem II (ϕ_{PSII}) in dark adapted leaves, calculated from F_oQ_A prior to the strong WL pulse and F_mWL during the pulse monitored by the Q_A flash of LIFT/FRR averages $\phi_{PSII}WL = 0.842 \pm 0.001$, ~5% larger than that obtained in the same dark adapted leaves from a saturating WL pulse of MINI-PAM ($\phi_{PSII}PAM = 0.798 \pm 0.002$; n = 22). This PAM-analogous strong WL pulse abolishes variable fluorescence and gives an average $\phi_{PSII}WL = 0.017 \pm 0.003$ (n = 21) implying that the pulse achieves >98% reduction of the PQ pool. Individual Q_A flash profiles after the WL pulse reveal a dramatic immediate disturbance of ETR during RQ_A phase of the transient (Fig. 2*f*). Tau 1 (ETR $Q_A \rightarrow$ PQ) slows immediately and takes ~15 s to return to dark values (Figs. 2*b*, and *f*). In contrast, the PQ pool becomes more reduced as τ_2 (ETR PQ $\rightarrow$ PSI) accelerates in response to the electron sink provided by the presence of light 1 in the WL pulse (Figs. 2*c,d, f*). Apparent PSII antenna size in the dark is shown in the box (Fig. 2*e*). Most parameters return to dark levels within 30 s following the WL pulse.

(iii) Dark to state 2 on addition of light 2

The transition from dark $\rightarrow$S2 is initiated with weak actinic light 2 from the (470 nm; 5 μmol photons m^{-2} s^{-1}, ~4 times stronger than the cumulative PFD in a Q_A flash). This weak light principally excites PSII and immediately produces a large, sharp initial transient increase in

356 $F'_mQ_A^{470}$ characteristic of photosynthetic induction, followed by a slow decline to dark levels
357 over the next 10 min (Fig. 2*a*). Concurrently, $F'Q_A^{470}$ increases some 30% above dark levels,
358 producing ~10% decline in $\phi'_{PSII}Q_A^{470}$ (Fig. 2*b*). Values of functional absorption cross-section
359 (σ'_{PSII}) follow the kinetics of F'_mQ_A and $F'Q_A$ (c.f., Figs. 2*a* and *e*) and are clearly evident in
360 the decrease of initial slopes of SQ_A phase of the Q_A flash (Fig. 2*g*).
361 Transfer to weak light 2 produces a RQ_A feature in the Q_A flash (Fig. 2*g*) similar to, but
362 less extreme than observed in the WL pulse (Fig. 2*f*) that is symptomatic of PQ pool over
363 reduction in the flash. Indeed the PQ pool immediately becomes more reduced (Fig. 2*c*) and the
364 RQ_A feature disappears over the next 10 min (Fig. 2*g*). Although much slower than τ_1, τ_2
365 transiently accelerates >3-fold on exposure to light 2 and contributes to the transient acceleration
366 and decline in ETR PQ → PSI (Fig. 2*d*). The "PQ pool/ST control loop" is displayed in real time
367 and despite partial re-oxidation, the PQ pool evidently remains sufficiently reduced (Fig. 2*c*) to
368 favour phosphorylation of a LHCII fraction in PSII that associates with PSI. Faster electron
369 transport to PSI (Fig. 2*d*) is indicative of the increasing electron sink in PSI following the ST and
370 increase in the light-harvesting capacity of PSI. Successive strong WL pulses in steady state
371 towards the end of the light 2 treatment abolish variable fluorescence (Fig. 2*g*) and deliver well
372 replicated values of F'_mWL^{470} and $\phi'_{PSII}{}^{470}$ (Figs. 2*a, b*) which are used to calculate $a'_{PSII}{}^{470}$ in
373 S2 (Fig. 2*e*; box).

374 *(iv) State 2 to state 1 on addition of light 1, and to state 2 on its removal*

375 The transition S2 to S1 is initiated by addition of light 1 (740 nm; 50 μmol photons m^{-2} s^{-1}) to
376 light 2 which remains present throughout the assay. The higher intensity of light 2 is applied to
377 accommodate the much lower leaf absorbance at this wavelength (Laisk *et al.* 2014). Light 1
378 immediately activates PSI as a strong electron sink and depresses $F'_mQ_A^{470+740}$ to an extent
379 comparable to that found when light 1 is applied in the dark (Fig. 2*a*) as can be seen in the Q_A

flash profiles (Figs. 2*f*, *h*). It also produces a small (~10%) decline in $F'Q_A^{470+740}$, so has relatively little effect on $\phi'_{PSII}{}^{470+740}$ (Fig. 2*b*).

Tau 1 accelerates by ~10% (Fig. 2*b*) but the PQ pool becomes more oxidised (Fig. 2*c*) and the rate of electron transfer to PSI accelerates two-fold, becoming stable after addition of light 1 (Fig. 2*d*). Values of σ'_{PSII} increase immediately and remain unchanged during the 10 min. exposure (Fig. 2*e*). The transition S2→S1 is clearly evident from the steady increase in $F'_mQ_A^{470+740}$ (highlighted by the double asterisk in Fig. 2*a*). Comparisons of the initial slopes of the decline in $F'_mQ_A^{470}$ during initial exposure to light 2, and again after removal of light 1, with the steady increase in $F'_mQ_A^{470+740}$ indicate that in *Arabidopsis npq*1 under these conditions, S1→S2 in light 2 is initially ~7 times faster than S2→S1 on addition of light 1.

On removal of light 1, but in the continued presence of light 2, F'_mQ_A increases immediately to levels of $F'_mQ_A^{470+740}$ well above those $F'_mQ_A^{470}$ at steady state in light 2 alone (Fig. 2*a*). The kinetic of subsequent decline in $F'_mQ_A^{470}$ and $F'Q_A^{470}$ replicates those observed initially but without the sharp induction transient. A strong WL pulse ~60 s after removal of light 1 (highlighted by an asterisk in Fig. 2*a*) produces a value for $F'_mWL^{470+740}$ that is clearly larger than F'_mWL^{470} (shown by the green broken line in Fig. 2*a*). Removal of light 1 also shows that the values of $\sigma'_{PSII}{}^{470+740}$ have increased well above those in light 2, and these again decline during the replication of S1→S2 (Fig. 2*e*). Steady state values of a'_{PSII} are shown in the boxes of (Fig. 2*e*) with largest values being found in S1.

Profound changes are observed in both phases of individual Q_A flashes when light 1 is removed to monitor a second S2→S1 (Figs. 2*h*). For example, in the SQ_A phase both F'_mQ_A and $F'Q_A$ increase within 3 s, as does σ'_{PSII} (indicated by the increased initial slope). Tau 1 accelerates slightly (Fig. 2*b*), the PQ pool immediately returns to the more reduced state previously prevailing in light 2 and tau 2 accelerates before resuming a transient response

identical to that in the first exposure to light 2 (Fig. 2*c*). Electron transfer to PSI slows to the rate attained at the end of the first exposure to light 2 (Fig. 2*d*). The kinetics of $F'_mQ_A^{470}$ and $\sigma'_{PSII}{}^{470}$ during the return from S1→S2 after removal of light 1 closely resemble those in the initial dark to S2 transition.

Probing "PQ pool/ST control loop" and other responses in ST assays of representative barley and Arabidopsis wild types and ST mutants

(i) Barley wild type and small antenna mutant chlorina-f2

Comparisons of pulse modulated chlorophyll fluorescence from barley wild type and its smaller antenna mutant *chlorina-f*2 is one of the earliest demonstrations of a genotype without ST (Chow *et al.* 1981) and so provide preliminary tests for the efficacy of LIFT/FRR analysis of ST. Compared to wild type, dark adapted sun-grown barley *chlorina-f2* monitored by LIFT/FRR in a strong WL pulse show ϕ_{PSII} = 0.77 ± 0.01 and 0.82 ± 0.01 (n = 5), respectively. Relative to wild type, σ'_{PSII} and a'_{PSII} in *chlorina-f2* are only 35% of wild type), consistent with a multiple deficiencies of LHCIIs (Harrison *et al.* 1993; Bossmann *et al.* 2007). All four ST criteria from LIFT/FRR assays confirm the absence of ST in antenna mutant *chlorina-f*2 (Table 1). In contrast, the extents of ST in wild type estimated from change in F'_mWL with fully reduced PQ, or in F'_mQ_A and functional (ϕ'_{PSII}) and optical absorption cross-sections (a'_{PSII}; apparent antenna size) with reduced Q_A, all confirm the presence of ST (Table 1). The latter three criteria are larger than those measured in a strong PAM-analogous WL pulse with fully reduced PQ pool. Comparisons of the relative oxidation state of the PQ pool (a key "PQ pool/ST control loop" parameter) show is more reduced (1.87 ± 0.12, n = 3) in wild type in light 2 and becomes more oxidized on addition of light 1 (4.48 ± 0.07, n = 4;). In contrast, there is little change in relative PQ pool oxidation state between light 2 (2.78 ± 0.10, n = 5) and light 2+1 (3.15 ± 0.26, n = 4) in *chlorina-f*2.

(ii) Arabidopsis wild type Col

Comparisons of the kinetic profiles of photosynthetic parameters in ST+ wild type *Col* with *ant*ST- *asLhcb*2-12 and *kin*ST- *stn*7/8 in Fig. 3 are colour-coded as in Fig. 2. At the outset, and as emphasized previously, exposure to light 1 in the dark is qualitatively similar in these genotypes (Figs. 3*a*, *f* and *k*), confirming that the rapid, reversible responses are not associated with the presence or absence of ST. Although sharp initial transients in $F'_mQ_A^{470}$ in the first ~1 to 2 min. of exposure to light 2 differ somewhat between genotypes (c.f., Figs. 3*a*, *f* and *k*) it is notable that they do not reappear in the replicate assay of S1→S2 after removal of light 1. In general, components of the "PQ pool/ST control loop" expose important and distinctive consequences leading to the absence ST following antenna LHCII depletion in *asLhcb*2-12 and the absence of STN kinase in *stn*7/8 (note that the strong WL pulse in the dark is applied at the end of the *stn7/8* assay; Fig. 3*k*).

The kinetics of photosynthetic parameters monitored in wild type *Col* (Figs. 3*a* - *e*) are rather similar to those observed in *npq*1 (Figs. 2*a* - *e*), but are also representative of *npq*4, *OEpsbs*, *pgr*5 *bkg* and *pgr5* (n = 14 experiments). As with the response to light 1 in the dark, the complex initial actinic response to added light 2 reports the induction of photosynthetic ETR. Strong WL pulses after 10 min. in light 2 produce well replicated values of F'_mWL^{470} (green broken line in Fig. 3*a*). Addition of light 1 produces an immediate drop in $F'_mQ_A^{470+740}$ comparable to that observed on addition of light 1 in the dark, but is followed by a steady increase throughout the 10 min. treatment tracing S2→S1(double asterisk). The ratio of the initial slope of F'_mQ_A in light 2 to that in light 2+1 indicates that the S2→S1 transition is ~4 faster than S1→S2 transition. The initial transient response of σ'_{PSII} to addition of light 2 follows the kinetic of fluorescence yields (c.f., Figs. 3*a* and *e*). As in *npq*1, estimates of optical

absorption cross section after 10 min. with added light 1 also give the largest values for a'_{PSII} in *Col* (Fig. 3*e*; box).

Turning to ETR kinetic profiles, addition of light 1 slightly accelerates τ_1 (Fig. 3*b*) but slows τ_2 as the PQ pool becomes more oxidized (Fig. 3*c*; double asterisk). The rate of electron transfer to PSI, however, is accelerated by light 1 (c.f., Figs. 2*d* and 3*d*). Changes in ETR parameters and PQ pool oxidation status in steady state are highly conserved in both wild types and their NPQ mutants (Table 2), implying that "PQ pool/ST control loop" operation is little influenced by factors sensitive to NPQ in these low PAR assays. Furthermore, there seem to be few differences that might be attributable to changes in photosynthetic carbon metabolism in these assays.

(iii) LHCII depleted antenna mutant asLhcb2-12

The traces of photosynhtetic parameters from the *ant*ST- mutant *asLhcb2-12* (n = 3) resemble those of *npq1* and *Col* (c.f., Figs. 3*a* - *e* and *f* - *j*). However, all LIFT/FRR criteria that support the presence of ST in *Col* and *npq1* confirm its absence in *asLhcb2-12* (Figs. 3*f* - *i*). Although the initial addition of light 2 to dark adapted *asLhcb2-12* produces discernable transients in $F'_mQ_A^{470}$ and $F'Q_A^{470}$ similar to those in ST+ genotypes (c.f., Figs. 3*a* and *i*), the slopes and amplitudes of these transients are much smaller. Again, replicate strong WL pulses at the end of the first exposure to light 2 yield reproducible values for F'_mWL^{470}. There is no increase in this parameter when the WL pulse is applied after 10 min. exposure to light 1 (red broken line in Fig. 3*f*) so EST_{WL} = 0.98 in this assay. There is no change in from $F_mQ_A^{470}$ to $F_mQ_A^{470+740}$ in light 2+1 (⊗ symbol in Fig. 3*f*) confirming the absence of S2→S1. Moreover, There is no detectable increase in σ'_{PSII} during the subsequent exposure to light 2+1 (⊗ symbol in Fig. 3*j*) and indeed a'_{PSII} declines. As previously reported (Osmond *et al.* 2017) values of

474 σ_{PSII} and a_{PSII} in this antenna mutant are ~20% smaller than those in *Col* (c.f., Figs. 3*e*; box
475 and 3*j*; box).

476 Otherwise, kinetic responses of ϕ'_{PSII}, ETR parameters (Figs. 3*g, h*) and the rate of
477 electron transfer to PSI represented by τ_2 / PQ_{OX} (Fig. 3*i*) are quite comparable to those in *Col* and
478 all ST+ genotypes (Table 2), although acceleration of τ_1 on addition of light 1 is somewhat
479 greater. Importantly, in *asLhcb*2-12 the PQ pool becomes more oxidized on addition of light 1,
480 just as it does in *npq*1 and *Col* (c.f., Fig. 2*c* and double asterisk in Figs. 3*c* and *h*). Elements of the
481 "PQ pool/ST control loop" are clearly functional in *asLhcb*2-12 but to little effect. The substantial
482 lack of mobilizable Lhcb2 substrates in the antenna of PSII in this mutant accounts for the
483 absence of ST, but compensatory adjustments in other LHCII complexes evidently confer near
484 normal ETR functions (Ruban *et al.* 2003, 2006), as discussed below.

485 *(iii) STN kinase mutant stn7/8*

486 In contrast, the traces from *stn*7/8 (Figs. 3*k* - *o*) and *stn*7 (data not shown) lacking *STN*7
487 kinases in LHCII-replete backgrounds show markedly different kinetic properties from those of
488 *npq*1, *Col* and *asLhcb*2-12. After the rapid, reversible response to light 1 in the dark, transfer to
489 light 2 leads to a large, persistent increase in $F'_mQ_A^{470}$ (Fig. 3*k*), almost identical to the level of
490 F'_mWL measured during the strong WL pulse in the dark (applied at the end of this assay). There
491 is scarcely any transient decline in $F'_mQ_A^{470}$ in light 2 so the fluorescence yield monitored in
492 steady state is essentially the same as when measured in a strong WL pulse (i. e., F'_mQ_A = 96 ±
493 2% F'_mWL; n = 9). Clearly this suggests that the PQ pool is strongly and constitutively reduced in
494 light 2 in these mutants, as confirmed by FRR model estimates of PQ_{OX} that are much less
495 responsive to addition of light 1 (Fig. 3*m*). In addition, there is a huge sustained increase in $F'Q_A$
496 that produces a substantially larger decline in $\phi'_{PSII}{}^{470}$ most of which is mitigated by addition of
497 light 1 (Fig. 3*l*). As in *asLhcb*2-12, there is no change in $F'_mQ_A^{470+740}$ following exposure to light

1 (⊗ symbol in Fig. 3*k*), consistent with the absence of S2→S1. In contrast to *npq*1, *Col*, and *asLhcb*2-12 but as in *asLhcb*2-12, $F_mQ_A^{470}$, $\sigma'_{PSII}{}^{470}$and $a'_{PSII}{}^{470}$ remain unchanged before and after 10 min. with added light 1 (Fig. 3*o*).

However, ETR parameters in the ST- genotypes also respond to ST assay light treatments in markedly different ways to *npq*1, *Col* and *asLhcb*2-12. In light 2 the time constants of τ_1 and τ_2 in *stn*7 and *stn*7/8 are twice as fast as in other genotypes (Table 2) while, as noted above, the PQ pool is substantially more reduced (asterisks in Fig. 3*l* and ⊗ symbol Fig. 3*m*). In fact, the PQ pool is reduced to about the same level as transiently achieved in strong WL pulses! Although addition of light 1 slows τ_1 to rates equivalent to those in other genotypes (⊗ symbol in Fig. 3*l*; Table 2) the PQ pool response to light 1 is much weaker than in *Col* and *asLhcb*2-12 (cf. Figs. 3*m* with 3*c*, *h*). The steady-state ratio of τ_2 / τ_1 in ST+ genotypes in light 2+1 and *asLhcb*2-12 is 7; in *stn*7 and *stn7/8* it is only 3.7 and the relative PQ pool oxidation level in light 2+1 is only half of that observed in the other genotypes (Table 2). Yet the response of the rate of electron transfer to PSI (represented by the ratio τ_2 / PQ_{OX}) is slowed by light 1 just as in the other genotypes (Fig. 3*n*). The absence of STN7 kinases in LHCII-replete *stn*7/8 (and *stn*7) clearly renders these genotypes ST- despite the high level of PQ pool reduction, indicating complex, but currently ill-defined alterations of photosynthetic electron transport properties between PSII and PSI.

Changes in functional and optical absorption cross-sections during ST

Functional absorption cross-sections measured in the dark (335 ± 13 $Å^2$/ RCII) and in S1 (340 ± 8 $Å^2$/ RCII) are well conserved overall in the six ST+ genotypes (*Col*, *npq*1, *OEpsbs*, *npq*4, *pgr*5 and *pg*5*bkg*), as are values of σ'_{PSII} in S2 (292 ± 10 $Å^2$/ RCII), reflecting the commonly held view that leaves are in S1 in the dark (Fig. 4*a*). Although σ'_{PSII} in two paired sets of NPQ+ and NPQ- genotypes (*Col* vs. *npq*1 and *OEpsbs* vs. *npq*4) and NPQ- *pgr*5 show similar response patterns, *pgr*5 *bkg* is an exception, inviting further evaluation. The low intensities of

470 nm and 740nm light used in ST have differential effects on steady state ϕ'_{PSII} and since $a'_{PSII} = \sigma'_{PSII} / \phi'_{PSII}$, the small changes in photochemical efficiency of PSII are responsible for the leveling of a'_{PSII} in dark and S2 (Fig. 4*b*). Unexpectedly, average optical cross-sections in the dark and S2 now are similar (a_{PSII} = 398 ± 16 and $a'^{470+740}_{PSII}$ = 404 ± 10 Å^2/PSII RC, respectively) and larger than in S1 (a'^{470}_{PSII} = 348 ± 12 Å^2/ RCII). The same two pairs of NPQ+ and NPQ- genotypes *Col* and *npq*1, *OEpsbs* and *npq*4, and *pgr*5 again show similar responses patterns but *pgr*5*bkg* remains an exception.

As expected (Andersson *et al.* 2003; Osmond *et al.* 2017), *ant*ST- *asLhcb*2-12 has a smaller optical absorption cross-section in the dark (~35% less than the mean of ST+ genotypes) and there is no change from dark to S2 and to S1 (Fig 4*b*). On the other hand, *kin*ST- *stn*7 and *stn*7/8, with dark a_{PSII} similar to the mean of ST+ genotypes, show a doubling of apparent antenna size in both light 2, and light 2+1 due to the much larger depression of ϕ'^{470}_{PSII} and $\phi'^{470+740}_{PSII}$ under the weak illumination conditions, but again, no evidence for a ST from σ'_{PSII} or a'_{PSII} (Figs. 4*a*, *b*).

Estimates of LHCII mobilization in ST monitored by F'_mQ_A and a'_{PSII} are three-times larger than from PAM-analogous estimates of F'_mWL

Yields of chlorophyll fluorescence in vivo at room temperature are commonly accepted to be proportional to the amount of antenna LHCII trimers associated with RCII. Thus all four fluorescence criteria in LIFT/FRR assays confirm there is no evidence for changes in LHCII trimer association with PSII in *asLhcb*2-12, *stn*7 and *stn*7/8 ST- genotypes of *Arabidopsis*; all are ST incompetent (Fig. 5). Six ST competent genotypes monitored with PAM-analogous WL pulses applied after steady states are attained in light 2 and light 2+1 give *EST* $_{WL}$ = 1.10 ± 0.02 (Fig. 5), implying ~10% decline in the LHCII pool associated with PSII during ST, similar to commonly cited values in the literature from PAM assays. Whereas these assays measure

546 chlorophyll fluorescence yield with fully reduced PQ, three other criteria, unique to LIFT/FRR
547 assays, that are based wholly or in part on chlorophyll fluorescence yields measured with
548 reduced Q_A, produce much larger estimates of the extent of ST. Those based on σ'_{PSII} alone are
549 near twice as large but values based on a'_{PSII} and on F'_mQ_A are more than three times larger
550 than traditional PAM-based estimates (Fig. 5).

551 The PAM-analogous assays are based on one or two values of $F'_mWL^{470+740}$ and two to
552 four values of F'_mWL^{470} from WL pulses in each experiment so potentially may be less sound
553 statistically than *EST* σ'_{PSII} and *EST* Q_A, based on the average of ~20 FRR fitted Q_A flashes at
554 steady state in each light treatment. Likewise, *EST* a'_{PSII} is calculated from values of σ'_{PSII}, but
555 also depends on values of $\phi'_{PSII}{}^{470}$ and $\phi'_{PSII}{}^{470+740}$ from WL pulses. These and other reasons for
556 the differences in the estimates in Fig. 5, and their implications, are explored in the discussion
557 below.

558 *Distinctive features of the RQ$_A$ phase of the Q$_A$ flash in* stn*7 and* stn*7/8*

559 Attention to individual Q_A flash profiles corresponding to key data points in the kinetic
560 traces from the above experiments assists interpretation of the kinetic profiles of ETR parameters
561 in ST assays. For example, the smaller value of σ_{PSII} in the *ant*ST- mutant *asLhcb2-12* (Fig. 3*j*)
562 is indicated by the shallower initial slope of the rise to F'_mQ_A (c.f., Figs. 6*a, c* and *b, d*) that
563 persists after 10 min. in light 2 and 10 min. after addition of light 1. As Fig. 6 reports features
564 emerging in the RQ_A phase beyond 10 ms it is convenient to use flashlet number, rather than
565 $\log_{10}$ ms for the *x*-axis, and data interpretation is aided by inclusion of values for τ_1, τ_2 and level
566 of PQ oxidation pertinent to each fluorescence transient profile.

567 All genotypes show a RQ_A phase feature during photosynthetic induction transient in the
568 first seconds of exposure to light 2 (Figs. 2*g*, and 6*a*, *c*, *e*) resembling that which relaxes within
569 14 s following the strong WL pulse in the dark (Fig. 2*f*). Previously ascribed to transient

over-reduction of PQ pool prior to the flash (Osmond *et al.* 2017), the numerical data (Figs. 6*a*, *c*, *e*) confirm the PQ pool is immediately more reduced 3 s after transfer to light 2. Addition of light 1 provides an extra sink for electron flow to PSI, immediately removing the RQ_A feature for the duration of the exposure to light 1 in *Col* and *asLhcb*2-12, but has little effect in *stn*7/8 (Figs. 6*e*, *f*). It returns rapidly after removal of light 1; in *Col* the level of PQ pool reduction 9 s after removal of light 1 is the same as that 3 s after transfer from dark to light 2 (c.f., numerical data in Figs. 6*b*, *a*).

The Q_A flash profiles in *asLhcb2-12* are similar to those of *Col* (Figs. 6*e*, *f*). The fluorescence yield in light 2 is smaller (consistent with its smaller antenna size) and the RQ_A feature also disappears after 10 min. in light 2 (c.f., Figs. 6*a*, *c*). Compared to *Col*, fluorescence yield in *asLhcb2-12* after 10 min. in light 2+1 declines much more rapidly on removal of light 1 (Fig. 6*d*). Although τ_1 does not change the PQ pool is more oxidised in *asLhcb*2-12 (c.f. numerical values in Fig. 6*d* vs. 6*b*), the processes balancing ETR and more rapid mitigation of PQ over-reduction in this genotype need further examination. As discussed below, they may reflect the 'concerted compensatory response of the light harvesting system' in this genotype (Ruban *et al.* 2006).

By contrast, in *stn*7/8 (and *stn*7) the RQ_A feature symptomatic of PQ pool over reduction persists throughout exposure to light 2 (Fig. 6*e*; curve L2 10 min.). It is not immediately abolished on addition of light 1 (Fig. 6*f*; curve L2+L1+3s). However, balanced ETR evidently does return after 10 min. in light 2+1 (Fig. 6*f*; curve L2+L110 min.) despite the absence of ST. It reappears immediately on removal of light 1 (Figs. 6*f*; curve L2-L1 9 s). These slower responses in *stn*7/8 are especially evident in normalised Q_A flash transients during relaxation from strong WL pulses applied to measure F'_mWL in light 2 and light 2+1 (data not shown). The persistent over-reduction of PQ pools in *stn*7/8 and *stn*7 under low levels of light 2 revealed here is generally in line with the conclusion of Tikkanen *et al.* (2010) that *stn*7/8 and *stn*7 mutants experience 'relative over excitation of PSII under low light'.

596

597 ## Discussion

598 *Validation of optical absorption cross-section changes during ST in situ*

599 The recent headline that 'State transitions are changes in optical absorption cross-section'
600 (Allen 2017), and the frequent loose use of this term since Wang and Myers (1974) suggests
601 this effort to measure a'_{PSII} (i. e., apparent antenna size) as parameter in ST is timely.
602 Starting with dark adapted leaves (presumably in S1) we transition to S2 by exposure to low
603 intensities of light 2 (470 nm) before addition of light S1 (740nm) to transition to S1, and
604 return to S2 on its removal; light 2 is present throughout. Chlorophyll fluorescence yield
605 with reduced Q_A (F'_mQ_A) and the functional absorption cross-section PSII (σ'_{PSII}) and other
606 parameters are measured in ~30 ms transient from 270 single turnover 1μs flashlets from the
607 Q_A flash protocol of LIFT/ FRR at 2 to 3s intervals (Osmond *et al.* 2017). The maximum
608 photochemical efficiency of PSII (ϕ'_{PSII}) during steady states in light 2 and light 2+1 is
609 monitored with the Q_A flash protocol during PAM-analogous strong WL pulses (~1 s). We
610 calculate $a'_{PSII} = \sigma'_{PSII} / \phi'_{PSII}$ (Kolber *et al.* 1998).

611 Four different criteria from these assays confirm the presence of, and reveal the
612 kinetics of, ST in wild type barley and *Arabidopsis* (as well its NPQ mutants) and the absence of
613 ST in barley *chlorina-f2* and in *asLhcb*2-12, *stn*7 and *stn*7/8 mutants of *Arabidopsis.* These
614 LIFT/FRR assays also furnish time constants for photosynthetic ETR components and
615 estimates of PQ pool redox state in each Q_A flash that provide insights into regulation of ST
616 kinetics in situ. Fitting the entire FRR model to chlorophyll fluorescence transient elicited by
617 the Q_A flash confirms rapid reduction of the PQ pool in light 2 and the acceleration of ETR
618 from PQ to PSII on addition of light 1; validating key components of the PQ pool/ST control
619 loop in situ.

Changes in optical absorption cross-section measured in leaves imply larger pools of LHCIIs may participate in ST than previously estimated

In light 2 the discrete antenna migration model for ST, based on 40 years of biochemical, biophysical and physiological data, specifies the reversible phosphorylation and mobilization of (P)LHCIIs pools PSII in stacked thylakoid membranes move to serve as antennae for PSI in unstacked stromal thylakoids (Fig. 1*a*). Literature estimates suggest from ~six to 20% of leaf LHCII pools may be involved (Haldrup *et al.* 2001; Rochaix 2014; c.f. Fig. 1*a*). Direct fluorescence spectromicroscopy of PSII and PSI in granal and stromal regions of chloroplasts in protoplasts from wild type *Arabidopsis* confirm 11 ± 2% of LHCIIs are mobilised during ST (Kim *et al.* 2015). Our spot measurements in PAM-analogous strong WL pulses monitored by the Q_A flash of LIFT/FRR are consistent with these estimates of LHCII mobilisation 8 ± 1% in barley wild type and 10 ± 2% in two wild types and four NPQ mutant genotypes of *Arabidopsis*.

In contrast, three criteria available from LIFT/FRR give much larger estimates of the extent of ST in the same assays. First, the functional absorption cross-section of PSII clearly distinguishes ST+ and ST- genotypes of *Arabidopsis* (*EST* σ'_{PSII} = 1.17 ± 0.02 vs. 1.00 ± 0.02; 17 ± 2% vs. 0 ± 2%, respectively). This signal is defined as 'the product of the light-harvesting capability of the light absorbing pigments and the efficiency of excitation transfer to the reaction center' (Kolber and Falkowski 1993) and is taken to indicate ST in phytoplankton at sea (Behrenfeld and Kolber 1999). Second, when σ'_{PSII} and ϕ'_{PSII} from a WL pulse in steady state light 1 and 2+1 are used to estimate optical absorption cross-section (a'_{PSII}; apparent antenna size of PSII; the "holy grail" of the present LIFT/FRR experiments) the implied extent of mobilisable LHCII in ST+ genotypes of *Arabidopsis* is even larger (*EST*$_{a'PSII}$ = 1.33 ± 0.03; 33 ± 3%). Third, three-fold larger estimates of LHCII mobilization are also obtained in ST+ genotypes simply by using fluorescence yield (F'_mQ_A) in light 2 and light 2+1as a criterion (*EST* $_{Q_A}$ = 1.35 ± 0.02;

644 35 ± 2%). All criteria also confirm the absence of ST in *chlorina-f2* of barley and *asLhcb*2-12 of
645 *Arabidopsis*, as well as the *Arabidopsis* STN7 kinase mutants *stn*7 and *stn*7/8.
646 Advances in fractionation of pigment-protein complexes in thylakoid membranes (e.g.,
647 Järvi *et al.* 2011) require the antenna migration model to be considered in the context of light-
648 dependent phosphorylation of most LHCIIs in chloroplasts under most illumination situations
649 (Tikkanen *et al.* 2011; Greico *et al.* 2015). These studies suggest that although the antenna
650 migration model and its "PQ pool/ST control loop" represents an acceptable central mechanism
651 for ST, much larger pools of (P) LHCIIs seem to participate in most aspects of the process. We
652 speculate that the larger values of implied LHCII participation in ST revealed by the Q_A flash of
653 LIFT/FRR may reflect chlorophyll fluorescence arising from the dynamics of a large pool of "free
654 (P)LHCIIs" loosely associated with RCIIs and perhaps portray their associations with a PSI-
655 LHCI-LHCII-PSII megacomplex in which rapid energy migration between the photosystems
656 occurs at room temperature (Yokono *et al.* 2015).
657 *Explanations for larger estimates of mobilizable LHCII pool from F'*$_m$*Q*$_A$ *and a'*$_{PSII}$ *from*
658 *LIFT/FRR*
659 Discrepancies between estimates of the extent of ST using different methods are not new. The
660 much recited report of 80% mobile LHCIIs during ST in *Chlamydomonas reinhardtii* based on
661 photoacoustic data overlooks an estimate of 10-20% mobile LHCII in the same experiments
662 based on then available immunochemical methods (Delosme *et al.* 1996). Although time
663 resolved fluorescence spectroscopy confirms ~10% of LHCII is mobilised during ST in this alga
664 (Ünlü *et al.* 2014), other multi-faceted analyses conclude that antenna size of PSII declines by
665 42% as that of PSI increases by 35% in wild type *C. reinhardtii* during transition from S1 to S2
666 (Nawrocki *et al.* 2016). Reconciliation of such differences requires integration of phenomena
667 monitored at biophysical, biochemical, structural, and/or physiological levels, each of which
668 depends on qualitatively different observations and thus can be expected to produce quantitatively
669 different estimates of the extents of ST.

The distinctive fluorescence parameters from the LIFT/FRR method used here give estimates of the extent of LHCII participation in ST that differ three fold in the same assay. In explaining these differences we re-emphasise that 'the FRR method is, in fact, a fluorescence induction curve' (Falkowski and Kolber 1995) and that the fluorescence level attained in the Q_A flash (F'_mQ_A) corresponds to F_J attained during the initial photochemical phase (O-J; 0.36 ms) of a Kautsky induction curve. When PAM analogous strong WL pulses are applied the fluorescence yield corresponds to that attained during the subsequent J-I-P thermal phase (J-I-P; >300 ms) of the curve (Stirbet and Govindjee 2012; Osmond *et al.* 2017; Keller *et al.* 2018). Arithmetically the larger estimates of the extent of ST (and by implication the larger LHCII pools involved) arise because they are calculated as % change in the lower fluorescence yields measured in the photochemical phase Q_A flash of LIFT. The smaller estimates obtained in ~1 s strong WL pulses that fully reduced the PQ pool arise because of the additional yield in the thermal phase of the O-J-I-P transient. This lowers the estimates of ST by a factor determined by the amplitude of fluorescence yield in the thermal phase relative to that in the photochemical phase.

This arithmetic explanation aside, the different estimates invite speculation as to whether different measures of chlorophyll fluorescence yield in situ, in the same assay provide insights into the functional and structural relationships among dynamic populations of pigment-protein complexes and PSII and PSI reaction centres during ST. In one such example, de Marchin *et al.* (2014) show 32% of the slower PSIIβ centres (2-3 times smaller antenna size) are converted to larger, faster PSIIα centres (PSII mega- and super complexes with a high degree of connectivity) in wild type *Chlamydomonas reinhardtii* during S2→S1. This conversion does not occur in the *stt*7 kinase mutant.

Possible functional and structural implications of differing estimates of the extent of ST

Functionally, there is agreement that fluorescence yield at F_J reports 'a temporarily stabilized Q_A reduction state, while electron donation by photochemistry and departure by $Q_A \rightarrow Q_B$ transition remain equal' (Laisk and Oja (2017). In contrast, consensus with respect to factors responsible for

the additional fluorescence arising in the thermal phase J-I-P during a strong WL pulse remains elusive. Stirbert and Govindjee (2012) suggest modulation 'in parallel with the reduction of Q_A, through changes at the PSII antenna and/or reaction centre, or, possibly through control of the oxidation-reduction of the PQ pool' may produce 'changes at the PSII antenna and/or reaction centre'. Schansker *et al.* (2014) and Keller *et al.* (2018) also consider that 'light-induced conformational changes in PSII centres' may be involved. Strong evidence that this might be so comes from our observation that ST incompetent *Arabidopsis* STN7 kinase mutants *stn*7/8 (and *stn*7) show little difference between the fluorescence yields of F'_mQ_A and F'_mWL. Suorsa *et al.* (2015) report, not surprisingly, that lacking the capacity to phosphorylate LHCs, *stn*7 thylakoids have low levels of 'extra' (P)LHCII, low levels of the major (P)LHCII-PSII complex (mc1) and lack the ST specific complex mc8 (PSI-LHCI-LHCII; Pesaresi *et al.* 2009). Such large structural changes and the persistent over-reduction of PQ pool in these mutants evidently prevent the Q_A flash from picking up F_J; in the absence of LHCII phosphorylation the transient mimics DCMU treatment.

Structurally, evidence now shows the original the discrete antenna migration model of ST comprises but a small part of the (P)LHCII pool in the light (Rantala *et al.* 2017). The 'LHCII connectivity model' for ST in *Arabidopsis* (Grieco *et al.* 2015) has up to 50% of LHCII trimers loosely associated with PSII super complexes (Galka *et al.* 2012) in an 'energetically connected LHCII lake' (Rantala and Tikkanen 2018). Known as 'extra (L)LHCIIs', Galka *et al.* (2012) and Wientjes *et al.* (2013*a*) propose this large pool is the source of (P)LHCIIs that attach to PSI centres to form the ST complex PSI-LHCI-LHCII-PSII (Pesaresi *et al.* 2009) in which excitation is transferred to PSI. Using delayed fluorescence spectroscopy at -196 ºC, Yokono *et al.* (2015) report that ~50% of PSII centres in leaves of *Arabidopsis* wild types, (and *stn*7 and *stn*7/8) are physically connected to PSI in a PSI-LHCI-LHCII-PSII megacomplex in which rapid energy migration between the photosystems occurs at room temperature.

Even though excitation transfer from the loosely associated 'extra (P)LHCIIs' to PSII centres is slower than from (P)LHCIIs to PSII centres connected to PSI in the ST complex (Wientjes *et al.* 2013*b*), it seems plausible that all members of the (P)LHCII population contribute to the yield of chlorophyll fluorescence monitored in the Q_A flash transient. Could the different extents of ST monitored by LIFT/FRR report fluorescence from differently connected members in this 'energetically connected LHCII lake' (Rantala and Tikkanen 2018) from which loosely associated (P)LHCIIs are recruited to PSII supercomplexes from which PSI-LHCI-LHCII-PSII megacomplexes are formed? In this context the largest values *EST* Q_A = 35 ± 0.02% and *EST* a'_{PSII} = 33 ± 0.03% (measured with reduced Q_A) might report fluorescence from the 'lake' as a whole. Because $\sigma'_{PSII} = a'_{PSII} \times \phi'_{PSII}$ could *EST* σ'_{PSII} = 17 ± 0.02% report a smaller population of PSII supercomplexes with more facile excitation transfer (P)LHCII-PSII? Does the smallest estimate, *EST* WL = 10 ± 0.02% (only obtained with fully reduced PQ) report the functionally effective ST configuration of the PSII-LHCII-LHCI-PSI megacomplex itself? Testing the plausibility of such speculative explanations for different estimates of (P)LHCII participation in ST clearly needs much closer expert examination. Clearly, the mechanistic details of (P)LHCII dynamics, from its association with PSII centres, its participation in PSII megacomplexes and the origins and extents of its mobilisation for association with PSI remain enigmatic. Nevertheless, we endorse the suggestion of Prášil *et al.* (2018) that 'the use of a combination of ST and MT flash protocols *(i.e., notation of Kolber et al. 1998 for the Q_A flash and WL pulse)* can provide a significant amount of information on PSII that would not otherwise be accessible from either protocol alone'.

Monitoring the "PQ pool / ST control loop" in ST+ and ST-genotypes

All of the above functional /structural speculation refers to steady states attained in light 2 and light 2+1 but the wealth of kinetic detail from Q_A flash transients should not be overlooked. For example, the kinetic of $F'_m Q_A$ shows S1→S2 is four to seven times faster than

S2→S1 but the latter is 2 orders of magnitude slower than the response of F'_mQ_A light 1 in the dark. Dietzel *et al.* (2011) report of S1→S2 /S2→S1 = 3.9 in PAM assays of low light grown *Col*. The kinetics of ETR in the RQ_A phase of the transient, and PQ_{OX} status from FRR model fit to the whole transient, adequately monitor the "PQ pool/ST control loop" in ST+ genotypes. On the other hand, although it is known that the deficiency of Lhcb1 and Lhcb2 in antennae of *asLhcb*2-12 (Andersson *et al.* 2003) is compensated by Lhcb5 homotrimers and heterotrimers Lhcb3 and 5 coupled to PSII (Ruban *et al.* 2003, 2006), these complexes are not phosphorylated and do not to serve as "substrates" for transfer to (or "attraction" for) PSI, thus rendering this genotype incapable of ST.

Nevertheless ETR and PQ_{OX} kinetics in *asLhcb*2-12 are remarkably similar to those of *Col* and other ST+ genotypes. Moreover, our holistic assays reveal that ~20% acceleration of ETR from PSII→PQ may help maintain PQox status in the face of up regulation of the LHCI content of PSI (Ruban *et al.* 2006) and show electron transport PQ → PSI is similar to ST+ genotypes. Interestingly, plants lacking Lhcb1 and 2 possess less spectrally distinct antennae (Ruban and Johnson 2009), an indication of compensatory adjustments helping to cope with the inability to perform ST'. More heterogeneous LHCII deficiencies in barley antenna mutant *chlorina-f2* (Harrison *et al.* 1993) also render this mutant genotype ST-. Evidence for wild type levels of Lhcb5, and a somewhat blue shifted 77° K emission spectrum (Bossmann *et al.* 1997), suggest a 'compensatory response in the light harvesting antenna' (Ruban *et al.* 2006) similar to that in *asLhcb*2-12, may be involved. Additional experiments are needed to explore our preliminary observations that *chlorina-f2* also may be less able to modulate PQ_{OX} status.

Lacking the ability to phosphorylate Lhcb1 and 2, *stn*7 also compensates for the absence of ST by up-regulation of PSI complexes under constant growth light (Grieco *et al.* 2012). This may explain why ETR parameters monitored by LIFT/FRR in *stn*7/8 (and *stn*7) in the dark do not differ from other genotypes, but in light 2 and on addition of light 1 both τ_1 and τ_2 are ~50%

771 faster than in *asLhcb2-12* and ST+ genotypes, and why the level of PQ pool reduction in the
772 presence of light 2 remains close to that attained in strong WL pulses. Indeed, Q_A flash profiles of
773 the *kin*ST- mutants reveal much slower relaxation of the RQ_A phase feature in light 2 and during
774 strong WL pulses, consistent with over-reduction of the PQ pool (Tikkanen *et al.* ??). Yet kinetic
775 profiles of the ratio of τ_2 to relative PQ oxidation (representing the rate of downstream electron
776 transport from PQH_2) differ little from those in other genotypes. Although there are no changes in
777 the apparent relative antenna size in *stn*7and *stn*7/8 between light 2 and light 2+1, the large
778 decline of ϕ'_{PSII} in these mutants at the low light intensities in the ST assays is unexpected. The
779 consequent doubling in a'_{PSII} implies that excitation absorbed by closed, nonfunctional PSII
780 centres is inevitably channeled to remaining open centers, thereby increasing their apparent
781 absorption cross section (Falkowski and Kolber 1995; Matsubara and Chow 2004).
782 In their seminal analysis of the dynamics of photosystem cross-sections during ST in
783 higher plants Ruban and Johnson (2009) conclude that 'invention of new experimental
784 approaches is likely to ignite a new wave of discoveries in this field'. The parameterization of
785 functional and optical cross-sections of PSII afforded by LIFT/FRR potentially offers one such
786 approach. Although the artificial light sources used here (and previously) to examine ST in
787 the laboratory in general do not match natural shade environments, new sources
788 (Hogewoning *et al.* 2012; Hirth *et al.* 2013) do effectively mimic natural canopy light
789 environments. Now that LIFT/FRR instruments fitted with a spectral radiometer sharing the
790 same optical path as the Q_A flash are available to monitor changes in spectral reflectance
791 with high time resolution (Wyber *et al.* 2017, 2018), it seems that an enriched understanding
792 of the roles of ST and sun flecks in photosynthesis in the shaded canopy is within reach.
793

794 **Acknowledgements**

795 This research was supported by a start-up grant from University of Wollongong to CBO that
796 facilitated development of the prototype LIFT instrument by Zbigniew S Kolber who also

advised on interpretation of data in this study. Studies of *Arabidopsis* genotypes in the Division of Plant Sciences, Australian National University with BJP were facilitated via the Australian Research Council (ARC) Centre of Excellence in Plant Energy Biology and by ARC grant DP120100872 to WSC. We thank Derek Collinge for germination and maintenance of *Arabidopsis* genotypes in controlled environment cabinets from seed provided by Eva-Mari Aro, Molecular Plant Biology University of Turku, Finland. Steve Dempsey and Gavin Pritchard maintained glasshouse cultivation of barley and avocado at ANU. The authors are grateful to John Allen and Shizue Matsubara for comments on early drafts of the MS, to Eva-Mari Aro, Mikko Tikkanen and Alexander Ruban for helpful discussions, and to three anonymous referees for encouraging reconsideration of our data in the context of recent research into structural and molecular mechanisms underlying ST.

References

Allen JF (2002) Plastoquinone redox control of chloroplast thylakoid protein phosphorylation and distribution of excitation energy between photosystems: discovery, background, implications. *Photosynthesis Research* **73**, 139–148

Allen JF (2017) Why we need to know the structure of phosphorylated chloroplast light-harvesting complex II. *Physiologia Plantarum* **161**, 28-44

Allen JF, Bennett J, Steinbeck KE, Arntzen CJ (1981) Chloroplast protein photophosphorylation couples plastoquinone redox state to distribution of excitation energy between photosystems *Nature* **291**, 21-25

Allen JF, Melis A (1988) The rate of P-700 photoxidation under continuous illumination is independent of State 1- State 2 transitions in the green alga *Scenedesmus obliquus*. *Biochimica et Biophysica Acta* 933, 95-106

821 Andersson J, Wentworth M, Walters RG, Howard CA, Ruban AV, Horton P, Jansson S (2003)
822 Absence of the Lhcb1 and Lhcb2 proteins of the light-harvesting complex of photosystem II-
823 effects on photosynthesis, grana stacking and fitness. *The Plant Journal* **35**, 350-361

824 Behrenfeld MJ and Kolber ZS (1999) Widespread iron limitation of phytoplankton
825 photosynthesis in the South Pacific Ocean. *Science* **283**, 840-843

826 Bennett J, Steinback KE, Arntzen, CJ (1980*)* Chloroplast phosphoproteins – regulation of
827 excitation-energy transfer by phosphorylation of thylakoid membrane polypeptides.
828 *Proceedings of the National Academy of Science USA* **77**, 5253-5257

829 Bonardi V, Pesaresi P, Becker T, Schleiff E, Wagner R, Pfannschmidt T, Jahns P, Leister D
830 (2005) Photosystem II core phosphorylation and photosynthetic acclimation require two
831 different protein kinases. *Nature* **437***,* 1179-1182

832 Bonaventura C, Meyers J (1969) Fluorescence and oxygen evolution from *Chlorella*
833 *pyrenoidosa*. *Biochimica et Biophysica Acta* **189**, 366-383

834 Bos I, Bland KM, Tian L, Croce R,Frankel LK, van Amerongen H, Bricker TM, Wientjes E
835 (2017) Multiple LHCII antennae can transfer energy efficiently to a single Photosystem I.
836 *Biochimica et Biophysica Acta* 1858, 371-378

837 Bossmann B Knoetzel J, Jansson S (1997) Screening *chlorina* mutants of barley (*H. vulgare* L.)
838 with antibodies against light-harvesting proteins of PSI and PSII: absence of specific antenna
839 proteins. *Photosynthesis Research* **52**, 127-136

840 Chow WS, Telfer A, Chapman DJ, Barber J (1981) State 1- State 2 transition in leaves and its
841 association with ATP-induced chlorophyll fluorescence quenching. *Biochimica et Biophysica*
842 *Acta* **638**, 60-68

843 Delosme R, Olive J, Wollman FA (1996) Changes in light energy distribution upon state
844 transitions: an invivo photoacoustic study of the wildtype and photosynthesis mutants from
845 *Chlamydomonas reinhardtii*. *Biochimica et Biophysica Acta* **1273**, 153-158

846 de Marchin T, Ghysels B, Nicolay S, Franck, F (2014) Analysis of PSII antenna size
847 heterogeneity of *Chlamydomonas reinhardtii* during state transitions. *Biochimica et*
848 *Biophysica Acta* **1837**, 121-130

849 Dietzel L, Bräutigam K, Steiner S, Schüffler K, Lepetit B, Grimm B, Schöttler MA,
850 Pfannschmidt T (2011) Photosystem II supercomplex remodelling serves as an entry
851 mechanism for state transitions in *Arabidopsis*. *The Plant Cell* **23**, 2964-2977

852 Falkowski PG, Kolber Z (1995) Variations in chlorophyll fluorescence yields in phytoplankton
853 in the world oceans. *Australian Journal of Plant Physiology* **22**, 341-355

854 Galka P, Santabarbara S, Khuong TTH, Degand H, Morosomme P, Jennings RC, Boekema EJ,
855 Caffarri S (2012) Functional analyses of the plant photosystem I-light-harvesting complex II
856 supercomplex reveal that light-harvesting complex II loosely bound to photosystem II is a
857 very efficient antenna for photosystem I in State II. *The Plant Cell* **24**, 2963-2978

858 Grieco M, Suorsa M, Paakkarinen v, Kangajarvi s, Aro E-M (2012) Steady-state
859 phosphorylation of light-harvesting complex II proteins preserves photosystem I
860 underfluctuating white light. *Plant Physiology* **160**, 1896-1910

861 Grieco M, Suorsa M, Jajoo A, Tikkanen M (2015) Light-harvesting II antenna trimers
862 connect energetically the entire photosynthetic machinery - including both photosystems
863 II and I. *Biochimica et Biophysica Acta* **1847**, 607-619

864 Haldrup A, Jensen PE, Lunde C, Scheller HV (2001) Balance of power: a view of the
865 mechanisms of photosynthetic state transitions. *Trends in Plant Science* **6**, 301-305

866 Harrison MA, Nemson JA, Melis A (1993) Assembly and composition of the chlorophyll *a* – *b*
867 light-harvesting complex of barley (*Hordeum vulgare* L.): Immunochemical analysis of
868 chlorophyll *b*-less and chlorophyll *b*-deficient mutants. *Photosynthesis Research* **38**, 141-151

869 Highkin HR (1950) Chlorophyll studies on barley mutants. *Plant Physiology* **25**, 294-306

870 Hirth M, Dietzel L, Steiner S, Ludwig R, Weidenbach H, Pfalz J, Pfannschmidt T (2013)
871 Photosynthetic acclimation responses of maize seedlings grown under artificial laboratory
872 light gradients mimicking natural canopy conditions. *Frontiers in Plant Science* **4**, 334 (12pp)

873 Horton P (1983) Control of chloroplast electron transport by phosphorylation of thylakoid
874 proteins. *FEBS Letters* **152**, 47-52

875 Hogewoning SW, Wientjes E, Douwstra P, Trouwborst G, van Ieperen W, Croce R, Harbinson J
876 (2012) Photosynthetic quantum yield dynamics; from photosystems to leaves. *The Plant Cell*
877 **24**, 1921-1935

878 Iwai M, Yokono M, Minagawa J (2008) Molecular remodeling of photosystem II during state
879 transitions in *Chlamydomonas reinhardtii*. *Plant Cell* **20**, 2177-2189

880 Iwai M, Yokono M, Minagawa J (2010) Live-cell imaging of photosystem II antenna
881 dissociation during state transitions. *Proceedings of the National Academy of Sciences USA*
882 **107**, 2377-2342

883 Järvi S, Suorsa M, Paakkarinen V, Aro E-M (2011) Optimized native gel systems for separation
884 of thylakoid protein complexes: novel super- and mega-complexes. *Biochemical Journal*
885 **439**, 207-214

886 Keller B, Vass I, Matsubara S, Paul K, Jedmowski C, Pieruschka R, Nedbal L, Rascher U,
887 Muller O (2018) Maximum fluorescence yield and electron transport kinetics determined by
888 light-induced fluorescence transients (LIFT) for photosynthesis phenotyping. *Photosynthesis*
889 *Research* https://doi.org/10.1007/s11120-018-0594-9

890 Kim E, Ahn TK, Kumazaki S (2015) Changes in antenna sizes of photosystems during state
891 transitions in granal and stroma-exposed thylakoid membrane of intact chloroplasts in
892 Arabidopsis mesophyll protoplasts. *Plant Cell Physiology* 56: 759-768

893 Kolber Z, Falkowski PG (1993) Use of active fluorescence to estimate phytoplankton
894 photosynthesis in situ. *Limnology and Oceanography* **38**, 1646-1665

895 Kolber Z, Klimov D, Ananyev G, Rascher U, Berry J, Osmond B (2005) Measuring
896 photosynthetic parameters at a distance: Laser Induced Fluorescence Transient (LIFT)
897 method for remote measurements of PSII in terrestrial vegetation. *Photosynthesis Research*
898 **84**, 121-129

899 Kolber Z, Prasil O, Falkowski PG (1998) Measurements of variable chlorophyll fluorescence
900 using fast repetition rate techniques: defining methodology and experimental protocols.
901 *Biochimica et Biophysica Acta* **1367**, 88-106

902 Laisk A, Oja V, Eichelmann H, Dall'Osto L (2014) Action spectra of photosystem II and I and
903 quantum yield of photosynthesis in leaves in State 1. *Biochimica et Biophysica Acta* **1837**,
904 315-325

905 Laisk A, Oja V (2017) Kinetics of photosystem II electron transport: a mathematical analysis
906 based on chlorophyll fluorescence induction. *Photosynthesis Research* **136**, 63-82

907 Ley AC, Mauzerall D (1982) Absolute absorption cross sections for photosystem II and the
908 minimum quantum requirement for photosynthesis in *Chlorella vulgaris*. *Biochimica et*
909 *Biophysica Acta* **680**, 95-106

910 Li X-P, Björkman O, Shih C, Grossman AR, Rosenquist M, Jansson S, Niyogi KK (2000) A
911 pigment-binding protein essential for regulation of photosynthetic light harvesting. *Nature*
912 **403**, 391-395

913 Li X-P, Müller-Moulė P, Gilmore AM, Niyogi KK (2002) PsbS-dependent enhancement of
914 feedback de-excitation protects photosystem II from photoinhibition. *Proceedings of the*
915 *National Academy of Sciences* USA **99**, 15222-15227

916 Matsubara S and Chow WS (2004) Populations of photoinactivated photosystem II reaction
917 centers characterized by chlorophyll *a* fluorescence lifetime in vivo. *Proceedings of the*
918 *National Academy of Sciences USA* **101**, 18234-18239

919 Mekala NR, Suorsa M, Rantala M, Aro E-M, Tikkanen M (2015) Plants actively avoid state
920 transitions upon changes in light intensity: role of light-harvesting complex II protein
921 dephosphorylation in high light. *Plant Physiology* **168**,721-734

922 Minagawa J (2011) State transitions-the molecular remodeling of photosynthetic
923 supercomplexes that controls energy flow in the chloroplast. *Biochimica et Biophysica Acta*
924 **1807**, 897-905

925 Munakage Y, Hojo M, Meurer J, Endo T, Tasaka M, Shikanai T (2002) PGR5 is involved in
926 cyclic electron flow around photosystem I and is essential for photoprotection in
927 *Arabidopsis*. *Cell* **110**, 361–371

928 Murata N (1969) Control of excitation transfer in photosynthesis I. Light-induced change of
929 chlorophyll *a* fluorescence in *Porphyridium cruenatum*. *Biochimica et Biophysica Acta* **172**,
930 242-251

931 Murata N (2009) The discovery of state transitions in photosynthesis 40 years ago.
932 *Photosynthesis Research* **99**, 155-160

933 Nawrocki WJ, Santabarbara S, Mosebach L, Wollman F-A, Rappaport F (2016) State transitions
934 redistribute rather than dissipate energy between two photosystems in Chlamydomonas.
935 *Nature Plants* 2, 16031

936 Niyogi KK, Grossman AR, Björkman O (1998) Arabidopsis mutants define a central role for
937 the xanthophyll cycle in regulation of photosynthetic energy conversion. *Plant Cell* **10**,
938 1121-1134

939 Osmond B, Chow WS, Wyber R, Zavaleta A, Keller B, Pogson BJ, Robinson SA (2017)
940 Relative functional and optical absorption cross sections of PSII and other photosynthetic
941 parameters monitored in situ, at a distance with a time resolution of a few seconds, using a
942 prototype light induced fluorescence transient (LIFT) device. *Functional Plant Biology* **44**,
943 985-1006

944 Pesaresi P, Hertle A, Pribil M, Kleine T, Wagner R, Strissel H, Ihnatowicz, Bonardi V,
945 Scharfenberg M, Schneider T, Pfannschmidt T, Leister D (2009) *Arabidopsis* STN7
946 kinase provides a link between short- and long-term photosynthetic acclimation. *The*
947 *Plant Cell* **21**, 2402-2423

948 Pfündel E (2007) JUNIOR-PAM chlorophyll fluorometer operators guide. H Walz GmbH,
949 Effeltrich, Germany, 58 pp.

950 Prášil O, Kolber ZS, Falkowski PG (2018) Control of the maximum chlorophyll fluorescence
951 yield by the Q_B binding site. *Photosynthetica* **56**, 150-162

952 Rantala M, Tikkanen M, Aro E-M (2017) Proteomic characterization of hierarchical
953 megacomplex formation in Arabidopsis thylakoid membrane. *The Plant Journal* **92**, 951-962

954 Rantala S, Tikkanen M (2018) Phosphorylation-induced lateral rearrangements of thylakoid
955 protein complexes upon light acclimation. *Plant Direct* 1-12

956 Rochaix J-D (2014) Regulation and dynamics of the light-harvesting system. *Annual Review of*
957 *Plant Biology* **65**, 287-309

958 Ruban AV, Wentworth M, Yakushevska AE, Keegstra W, Lee PJ, Dekker JP, Jansson S,
959 Boekema E, Horton P (2003) Plants lacking the main light-harvesting complex retain
960 photosystem II macro-organisation. *Nature* **421**, 648-652

961 Ruban AV, Solovieva S, Lee PJ, Iiloaia C, Wentworth M, Ganeteg U, Klimmek F, Chow WS,
962 Anderson JM, Jansson S, Horton P (2006). Plasticity in the composition of the light-
963 harvesting antenna of higher plants preserves structural integrity and biological function.
964 *Journal of Biological Chemistry* **281**, 14981-14990
965 Ruban AV, Johnson MP (2009*)* Dynamics of higher plant photosystem cross-section associated
966 with state transitions. *Photosynthesis Research* **99**, 173-183
967 Schansker G, Tóth SZ, Holzwarth AR, Garab G (2014) Chlorophyll *a* fluorescence: beyond the
968 limits of the Q_A model. *Photosynthesis Research* **120**, 43-58
969 Stirbet A, Govindjee (2012) Chlorophyll a fluorescence induction: a personal perspective of the
970 thermal phase. *Photosynthesis Research* **113**, 15-61
971 Suggett DJ, MacIntyre HL, Geider RJ (2004) Evaluation of optical determinations of light
972 absorption of photosystem II in phytoplankton. Limnolo*gy and Oceanography: Methods* **2**,
973 316-332
974 Suorsa M, Rantala M, Mamedov F, Lespinasse M, Trotta A, Grieco M, Vuorio E, Tikkanen M.
975 Jävi S, Aro E-M (2015) Light acclimation involves dynamic re-organisation of the pigment-
976 protein megacomplexes in non-appressed thylakoid domains. *The Plant Journal* **84**, 360-373
977 Tikkanen M, Nurmi M, Suorsa M, Danielsson R, Mamedov F, Styring S, Aro E-M (2008)
978 Phosphorylation-dependent regulation of excitation energy distribution between two
979 photosystems in higher plants. *Biochimica et Biophysica Acta* **1777**, 425-432
980 Tikkanen M, Grieco M, Kangasjärvi, Aro E-M (2010) Thylakoid protein phosphorylation in
981 higher plant chloroplasts optimises electron transfer under fluctuating light. *Plant Physiology*
982 **152**, 723-735
983 Tikkanen M, Grieco M, Aro E-M (2011) Novel insights into light-harvesting complex II
984 phosphorylation and 'state transitions'. *Trends in Plant Science* **16**, 126-131

985 Tikkanen M, Aro E-M (2014) Integrative regulatory network of plant thylakoid energy
986 transduction. *Trends in Plant Science* **19**, 10-17

987 Ünlü C, Drop B, Croce R, van Amerongen H (2014) State transitions in *Chlamydomonas*
988 *reinhardtii* strongly modulate the functional size of photosystem II but not of photosystem I.
989 *Proceedings of the National Academy of Sciences USA* **111**, 3461-3465

990 Wang RT, Myers J (1974) On the state 1-state 2 phenomenon in photosynthesis. *Biochimica et*
991 *Biophysica Acta* **347**, 134-140

992 Wientjes E, van Amerongen H, Croce R (2013 *a*) LHCII is an antenna of both photosystems
993 after long term acclimation. *Biochimica et Biophysica Acta* **1827**, 420-428

994 Wientjes E, van Amerongen H, Croce R (2013 *b*) Quantum yield of changes in photosystem II:
995 effect of changes in antenna size upon light acclimation. *Journal of Physical Chemistry* B
996 **117**, 11200-11208

997 Wientjes E, Drop B, Kouřil R, Boekema EJ, Croce R (2013 *c*) During state 1 to state 2 transition
998 in Arabidopsis thaliana, the photosystem II supercomplex gets phosphorylated but does not
999 disassemble. *Journal of Biological Chemistry* **288,** 32821-32826

1000 Wyber RA, Malenovsky Z, Ashcroft MB, Osmond B, Robinson SA (2017) Do daily and
1001 seasonal trends in leaf solar induced fluorescence reflect changes in photosynthesis, growth
1002 or light exposure? *Remote Sensing* **9** (604): 1-19

1003 Wyber RA, Osmond B, Ashcroft MB, Malenovsky Z, Robinson SA (2018) Remote monitoring
1004 of dynamic canopy photosynthesis with high time resolution light-induced fluorescence
1005 transients. *Tree Physiology* **38**, 1302-1318

1006 Yokono M, Takabayashi A, Akimoto S, Tanaka A (2015) A megacomplex composed of both
1007 photosystem reaction centres in higher plants. *Nature Communications* **6**, 6675

1008

Table 1: All four criteria from LIFT/FRR assays confirm the absence of ST in the small antenna mutant *chlorina-f2* of barley. In contrast, the estimated extents of ST in wild type from change in functional (σ'_{PSII}) or optical absorption cross-sections (a'_{PSII}; apparent antenna size) with reduced Q_A are three-fold larger than those measured from F'_mWL in a strong PAM-analogous WL pulse with fully reduced PQ pool (means ± SE; n = 5).

Genotype and light treatment	F'_mWL	F'_mQ_A	σ'_{PSII}	a'_{PSII}
			Å²/PSII RC	
Barley *chlorina-f2*				
10 min. light 2	1306 ± 62	561 ± 29	109 ± 1	143 ± 2
10 min. light 2+1	1328 ± 65	566 ± 30	110 ± 1	146 ± 3
Extent of ST	**1.02 ± 0.02**	**1.01 ± 0.01**	**1.01 ± 0.01**	**1.02 ± 0.01**
Barley wild type				
10 min. light 2	2274 ± 147	1762 ± 136	295 ± 8	408 ± 12
10 min. light 2+1	2379 ± 157	1931 ± 159	339 ± 10	475 ± 14
Extent of ST	**1.05 ± 0.01**	**1.09 ± 0.02**	**1.15 ± 0.00**	**1.16 ± 0.01**

Table 2: Steady state values of electron transfer parameters in *Arabidopsis* genotypes in response to light treatments during ST assays, as estimated from the first 10 ms in the RQ_A phase of Q_A flash transients. Values in bold italic among ST- mutants identify parameters that differ markedly from those of ST+ genotypes (3 to 6 biological replicates; mean ± SE of ~20 Q_A flashes).

Genotype	Light treatment	ETR $Q_A \rightarrow PQ$ τ_1 (ms)	PQ pool oxidation status (relative)	ETR $PQ \rightarrow PSI$ τ_2 (ms)
State transitions present (ST+)				
*Col, pgr*5 *bkg*	**dark**	0.80 ± 0.01	3.64 ± 0.14	6.51 ± 0.30
	L2	0.84 ± 0.01	2.39 ± 0.15	3.64 ± 0.08
	L2 +L1	0.72 ± 0.02	7.05 ± 0.35	4.68 ± 0.30
	L2	0.79 ± 0.02	2.10 ± 0.25	3.12 ± 0.28
*OEpsbs, npq*1, *npq*4	**dark**	0.76 ± 0.02	4.14 ± 0.18	7.44 ± 0.27
	L2	0.81 ± 0.01	2.70 ± 0.16	3.83 ± 0.10
	L2 +L1	0.72 ± 0.01	6.50 ± 0.21	5.31 ± 0.13
	L2	0.74 ± 0.02	1.90 ± 0.27	2.91 ± 0.27
*pgr*5	**dark**	0.82 ± 0.01	4.10 ± 0.14	7.27 ± 0.28
	L2	0.84 ± 0.05	2.69 ± 0.05	3.71 ± 0.14
	L2 +L1	0.75 ± 0.01	6.77 ± 0.13	4.77 ± 0.10
	L2	0.83 ± 0.01	2.49 ± 0.35	3.52 ± 0.30
State transitions absent (ST-)				
asLhcb2-12	**dark**	0.72 ± 0.01	3.98 ± 0.16	6.92 ± 0.37
	L2	0.78 ± 0.01	2.79 ± 0.17	3.90 ± 0.07
	L2 +L1	***0.63 ± 0.01***	6.27 ± 0.10	4.57 ± 0.20
	L2	0.76 ± 0.01	2.75 ± 0.08	3.70 ± 0.06
stn7, stn7/8	**dark**	0.79 ± 0.02	4.06 ± 0.15	6.18 ± 0.15
	L2	***0.41 ± 0.02***	***1.09 ± 0.01***	***1.80 ± 0.03***
	L2 +L1	0.72 ± 0.01	***3.27 ± 0.31***	***2.72 ± 0.20***
	L2	***0.39 ± 0.02***	***1.08 ± 0.01***	***1.71 ± 0.03***

Figure 1: (*a*) A schematic summary of the antenna migration model for state transitions structured to correspond with the assay protocol used here. Photosynthetic parameters from PAM and LIFT/FRR in the boxes are colour-coded corresponding to blue light 2 (λ 470 nm) and to magenta after addition of near far red (λ 740 nm) light 1 from LED sources to bring about state transitions to S1→S2 and S2→S1. This colour coding is applied to kinetic traces of all parameters to delineate responses to these light treatments in subsequent Figures.

(*b*) Colour-coded state transition assay of a dark adapted spinach leaf monitored with the weak modulated red light measuring beam (MB) of MINI-PAM with saturating white light pulses (SP). After a pulse to measure F_mPAM in the dark, transition to S2 is initiated with weak light 2 (470 nm). After ~10 min. steady state chlorophyll fluorescence yield in S2 is attained and another strong WL pulse is given to measure F'_mPAM^{470}. Light 2 is retained throughout the assay when light 1 (740 nm) is added to initiate transition to S1. Light 1 is removed after ~10 min. and shortly thereafter another WL pulse is given to measure $F'_mPAM^{470+740}$. The extent of the state transition (*EST* PAM) is calculated from $F'_mPAM^{470+740}$ / F'_mPAM^{470}. LIFT/FRR assays follow a similar sequence, but additionally, another WL pulse is applied ~10 min. after removal of light 1 to replicate F'_mWL^{470}.

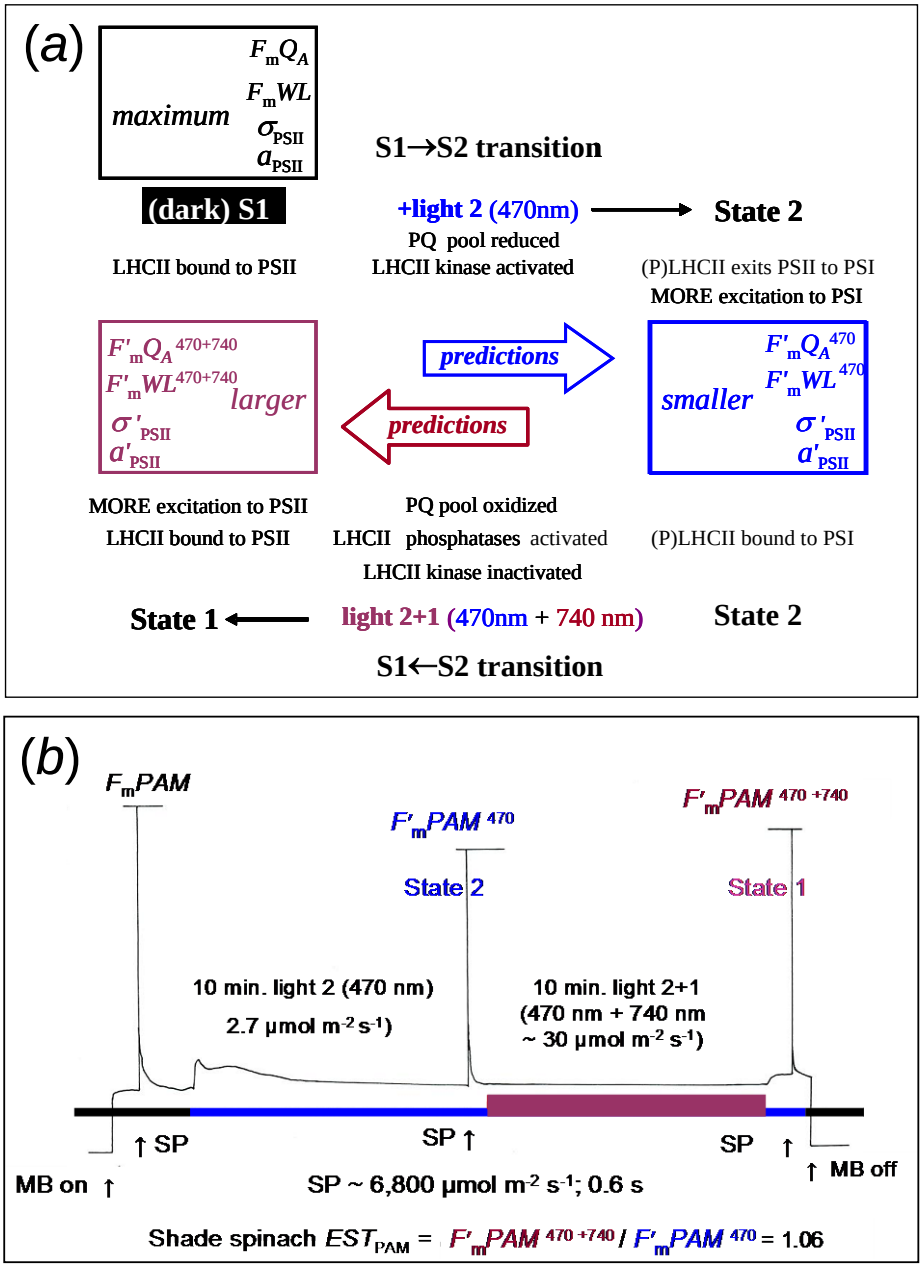

Figure 2: Colour-coded kinetic profiles in *Arabidopsis* NPQ mutant *npq*1 (violaxanthin de-epoxidase depleted) assayed with the Q_A flash of LIFT/FRR (*a* - *e*) annotated with the nomenclature of Osmond *et al.* (2017). Each data point is derived from FRR model fit to a Q_A flash transient performed at intervals of 2 to 3 s, representative examples of which are illustrated (*f* - *h*).

(*a*) Steady state chlorophyll fluorescence in the dark adapted leaf declines during ~1 min. in light 1 (F_mQ_A; red trace) whereas intrinsic yield does not (F_oQ_A; open red symbols). Maximum fluorescence yield (F_mWL) and photochemical efficiency of PSII (ϕ'_{PSII}) are obtained in a subsequent strong WL pulse. The transition from dark to S2 is initiated by ~10 min. exposure to light 2 and monitored by the kinetic of $F'_mQ_A^{470}$ (blue trace), after which a strong WL pulse is repeated twice to monitor maximum yield in S2 (F'_mWL^{470}). Addition of light 1 for ~ 10 min (in the presence of light 2) brings about S2→S1, the kinetic of which is reflected in the slope of $F'_mQ_A^{470+740}$ (double asterisk, magenta trace) which also is monitored in a strong WL pulse shortly after removal of light 1 (asterisk). A second estimate of S2 is obtained with another pulse in light 2 ~ 10 min. after removal of light 1.

(*b*) Colour-coded $\phi'_{PSII}Q_A$ (line) and τ_1 (kinetics of ETR $Q_A \rightarrow$ PQ; open symbols) and

(*c*) Relative oxidation status of the PQ pool (line) and τ_2 (kinetic of PQ pool re-oxidation; open symbols).

(*d*) Time constant of electron transport from PQ to PSI calculated by scaling the time constant of PQ pool re-oxidation with the size of the oxidized portion of the PQ pool.

(*e*) Functional (σ'_{PSII}) absorption cross-section of PSII. Colour-coded boxes show steady state values of optical absorption cross-section (a'_{PSII}; $Å^2$/ RCII) in the dark, in S2 and S1.

(*f* - *h*) Representative Q_A flash profiles at key time points. The time base is switched to $\log_{10}$ µs in the first 10 ms of the RQ_A transient to clarify changes in ETR parameters.

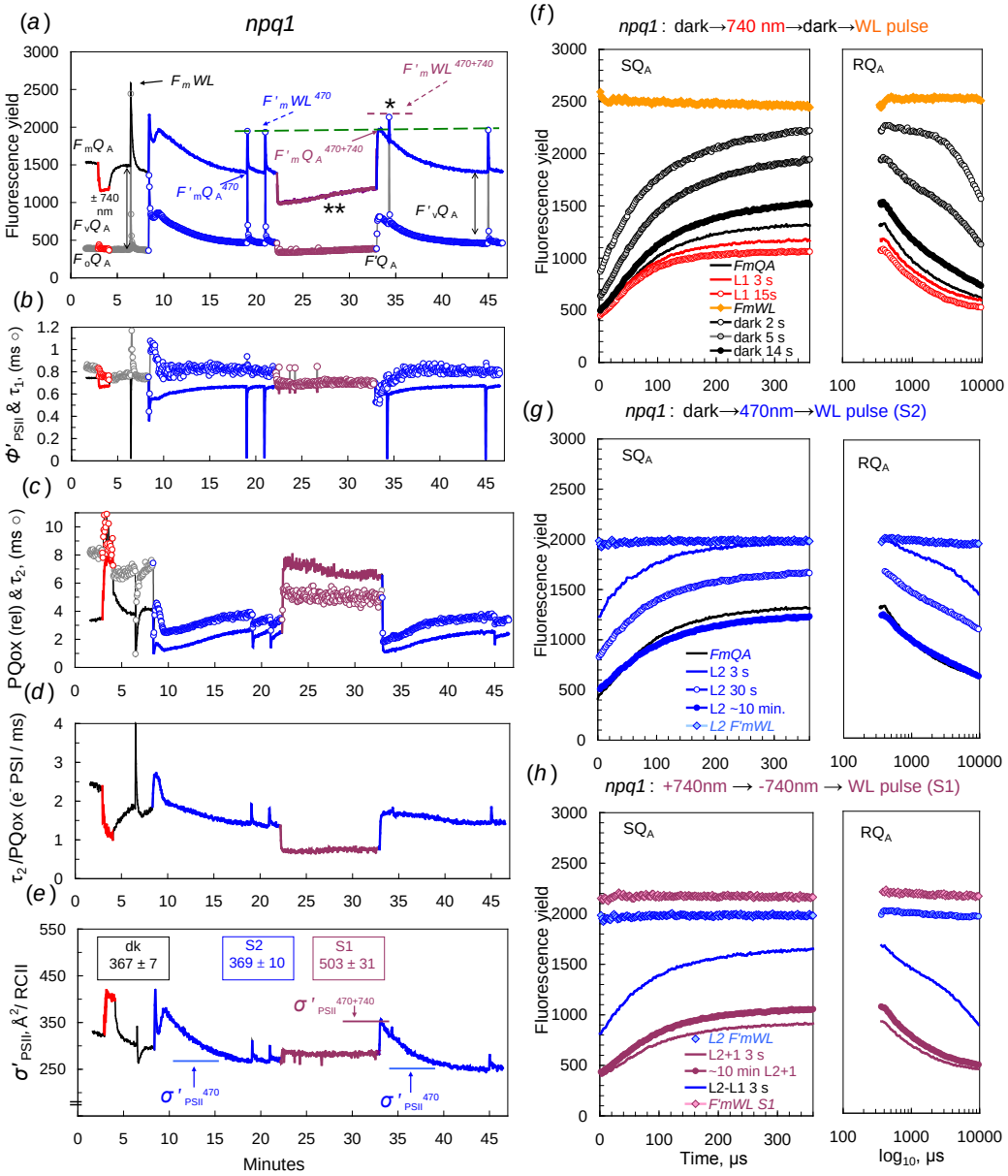

Figure 3: Representative LIFT/FRR assays with notation and colour-coding as in Fig. 2 showing (*a* - *e*) ST+ *Arabidopsis* wild type *Col*, (*f* - *j*) *ant*ST- LHCII mutant *asLhcb*2-12, and (*k* - *o*) *kin*ST- STN7 kinase mutant *stn*7/8 (N.B. no WL pulse in the dark).

The presence of ST in *Col* is shown by an increase in $F'_mWL^{470+740}$ (asterisk in *a*) compared to F'_mWL^{470}, (highlighted by green broken line). On this criterion (red broken lines) ST are absent in *asLhcb*2-12 (*f*), and *stn*7/8 (*k*). These distinctions are further confirmed by three other criteria:

(i) F'_mQ_A kinetic in light 2+1 highlighted by the double asterisk in (*a*) and red ⊗ symbols showing no change in (*f*) and (*k*),

(ii) increase in σ'_{PSII} (broken lines) in (*e*) that is absent in (*j*) and (*o*), and

(iii) increase in steady state values of a'_{PSII} associated with ST in *Col* (*e*) that is not evident in *asLhcb*2-12 or *stn*7/8 (red ⊗ symbols, *j* and *o*).

The contrasting dynamic responses of τ_1, τ_2 and relative oxidation state of the PQ pool to light 2 and light 2+1 in *Col* (*b*, *c*) and *asLhcb*2-12 (*g*, *h*) compared with those in *stn*7/8 (*l*, *m*), as well as uniformity of electron flow PQ to PSI (*d*, *i*, *n*) are discussed in the text.

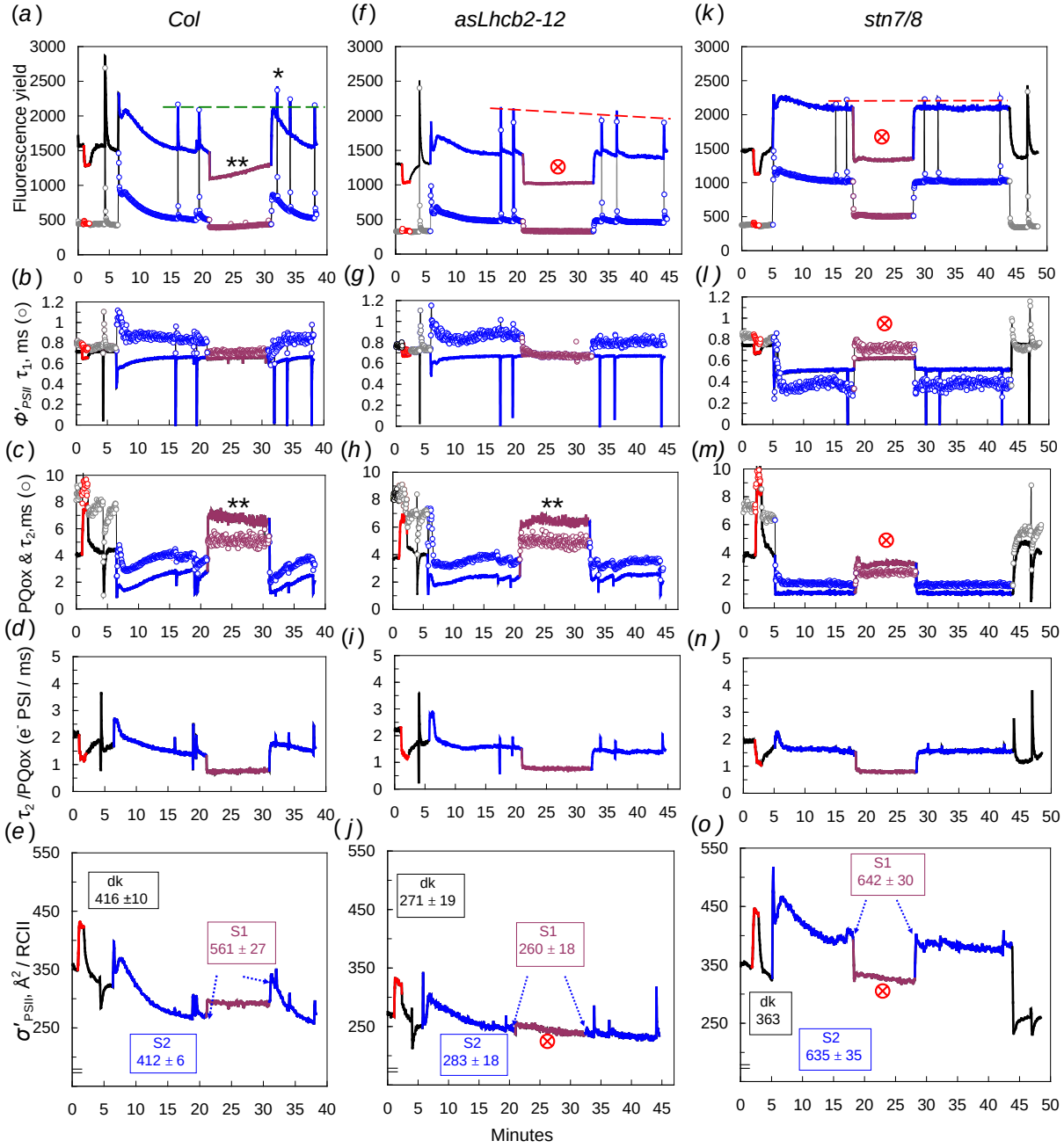

Figure 4: Functional absorption cross-section (*a*) and (*b*) optical absorption cross-section (apparent antenna size) in *Arabidopsis* genotypes at steady state in the dark, after ~10 min. in light 2 (S2) and soon after 10 min. in light 2+1 (S1). Values of a'_{PSII} are calculated from σ'_{PSII} / ϕ'_{PSII} (means ± SE; n = 2 to 8; no error bars indicates duplicate measurements).

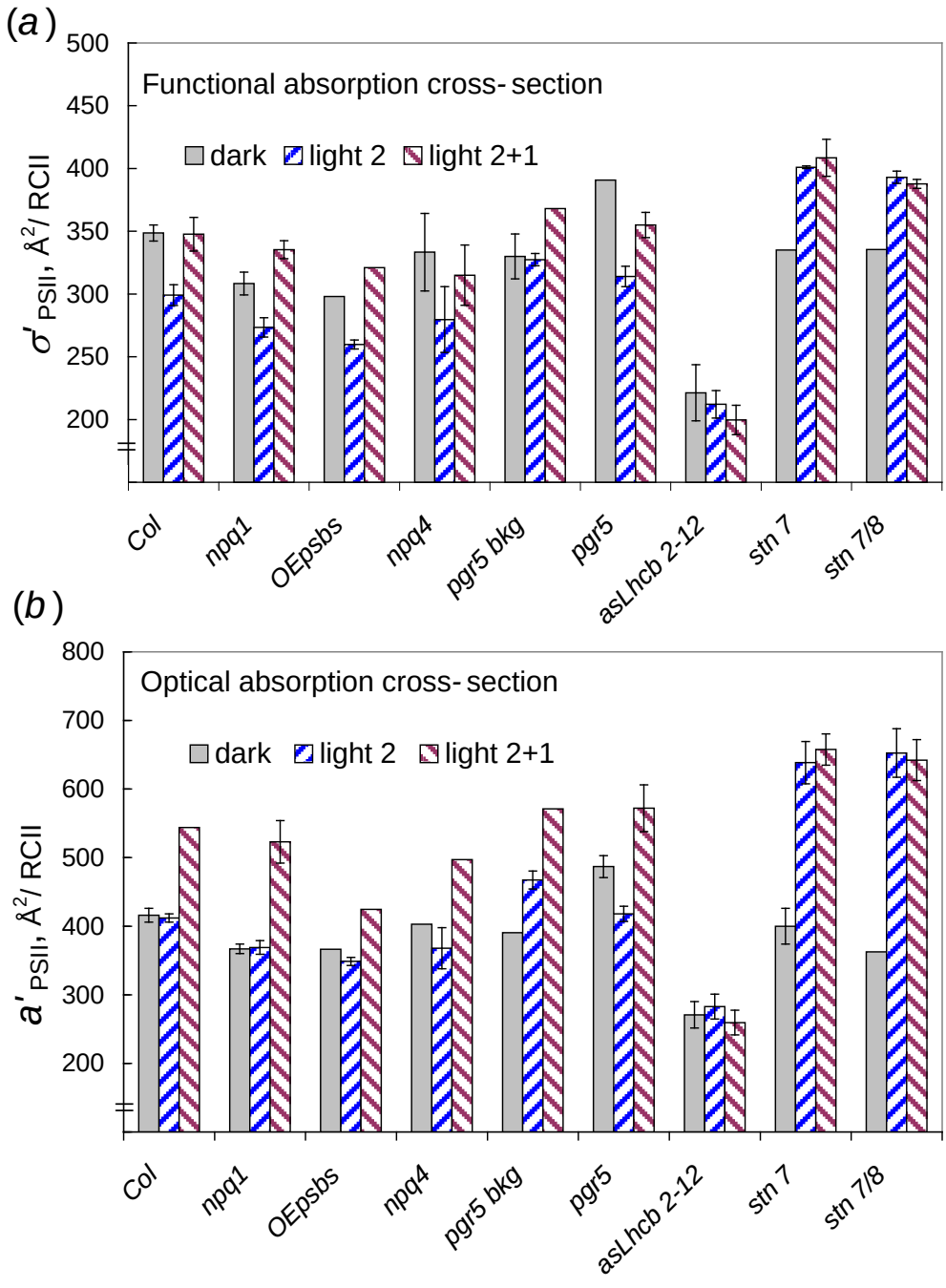

Figure 5: Estimates of the mobile fraction of LHCII pools implied from the extents of ST from four chlorophyll fluorescence criteria from the Q_A flash of LIFT/FRR. The criterion F'_mWL is obtained from strong WL pulses (fully reduced PQ pool) and the other three criteria are obtained with reduced Q_A. Data are averages (± SE) from a total of 22 assays of six ST competent *Arabidopsis* genotypes (ST+) and a total of seven assays of three ST incompetent genotypes (ST-).

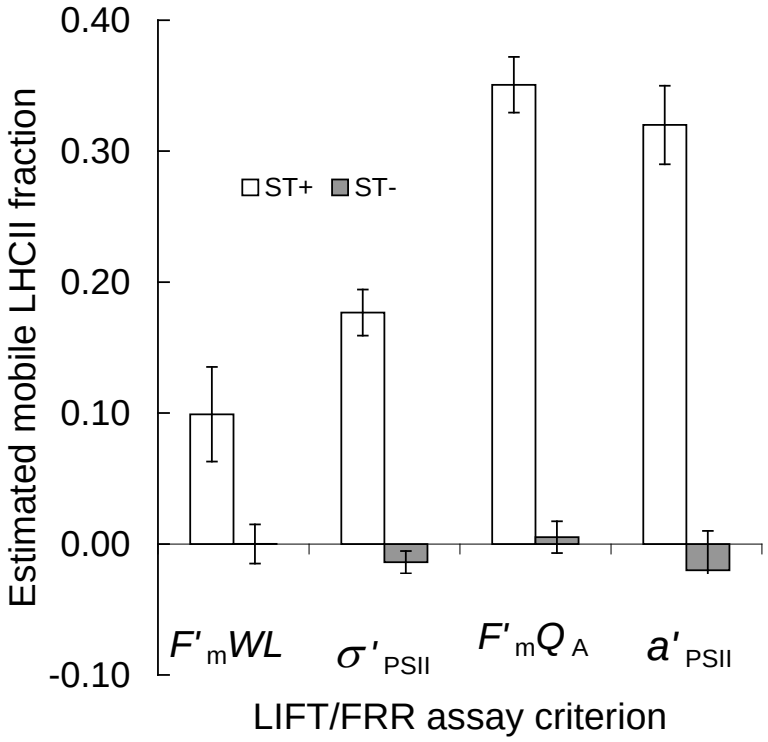

Figure 6: Entire Q_A flash transients (on the basis of flashlet number) at important time points during the ST assays shown in Fig. 3. Numbers in parenthesis refer to τ_1 and τ_2 (ms) and the relative oxidation state of the PQ pool, respectively, obtained from FRR model fit to the first 10 ms of the RQ_A phase (indicated red data point) in each transient. The persistently slower relaxation of the RQ_A feature in *stn*7/8 after 10 min in light 2 (*e*), and on addition and removal of light 1(*f*) are highlighted with ⊗ symbols.